Università di Genova

DEPARTMENT OF EXPERIMENTAL MEDICINE

PhD COURSE IN EXPERIMENTAL MEDICINE

Curriculum of Biochemistry

"Role of LANCL1 and LANCL2 in the physiology and biochemistry of myocytes and cardiomyocytes."

Candidate: Giulia Begani

Tutor: Prof.ssa Elena Zocchi

Prof.ssa Laura Sturla

PhD Program Coordinator

Prof. Ernesto Fedele

Academic Year 2021-2022

XXXV Cycle

A Laura, Anima pura e Roccia

INDEX

FIGURES INDEX

TABLES INDEX

ABBREVIATIONS

A

Abscisic Acid

AC: Adenylyl Cyclase

AKT: Protein Kinase B

AMPK: 5' Adenosine Monophosphate-activated Protein Kinase

AT: Adipose Tissue

ATCC: American Type Culture Collection

AUC: Area Under the Curve

B

BAT: Brown Adipose Tissue

BW: Body Weight

C

cADPR: Cyclic ADP-Ribose

cAMP: Cyclic Adenosine Monophosphate

CICR: Calcium-Induced Calcium Release

CMV: Cytomegalovirus

CO_2: Carbon Dioxide

CREB: cAMP Response Element-Binding Protein

D

DMEM: Dulbecco's Modified Eagle Medium

dNTPs: Deoxynucleotide Triphosphate

E

ECL: Enhanced Chemiluminescence

EDTA: Ethylenediaminetetraacetic Acid

ELISA: Enzyme-Linked Immunosorbent Assay

ERs: Estrogen Receptors

ERRs: Estrogen-Related Receptors

F

FBS: Fetal Bovine Serum

FDA: Food and Drug Administration

FDG: Fluorine-18 Deoxyglucose

G

GaPDH: Glyceraldehyde 3-Phosphate Dehydrogenase

GDM: Gestational Diabetes Mellitus

GFP: Green Fluorescent Protein

GLP-1: Glucagon-Like Peptide 1

GLUT1: Glucose Transporter 1

GLUT4: Glucose Transporter 4

GLY: Glycine

GPCR: G Protein-Coupled Receptor

GRs: Glucocorticoid Receptors

GRAS: Generally Recognized as Safe

GST: Glutathione S-Transferase

J

JC-1: Tetraethylbenzimidazolylcarbocyanine iodide

K

Kd: Dissociation Constant

KO: Knock Out

KRH: Krebs-Ringer-HEPES-Glucose-Glutamine Buffer

L

LANCL: LanC-Like

M

mTORC: Mammalian Target of Rapamycin Complex 1

N

NAD: Nicotinamide Adenine Dinucleotide

NAMPT: Nicotinamide Phosphoribosyl Transferase

NBDG: 2-[N-(7-Nitrobenz-2-oxa-1,3-diazol-4-yl)amino]-2-deoxy-D-glucose

NO: Nitric Oxide

O

O_2: Oxygen

OGTT: Oral Glucose Tolerance Test

P

p-AMPK: Phospho-5' Adenosine Monophosphate-Activated Protein Kinase

PBS: Phosphate Buffered Saline

PBST: Phosphate Buffered Saline Tween

PCR: Polymerase Chain Reaction

PDH: Pyruvate Dehydrogenase Complex

PET: Positron Emission Tomography

PFK1: Phosphofructokinase-1

PGC-1a: Peroxisome Proliferator-Activated Receptor Gamma Coactivator 1-alpha

PGE_2: Prostaglandin E2

PIC: Protease Inhibitor Cocktail

PKA: Protein Kinase A

PTX: Pertussis Toxin

PYLs: PYR1-Like

PYR1: Pyrabactin Resistance1

R

RT-PCR: Real Time Polymerase Chain Reaction

RCF: Relative Centrifugal Force

RCAR: Regulatory Components of ABA Receptors

ROI: Regions Of Interest

ROS: Reactive Oxygen Species

S

SD: Standard Deviation

SDS-PAGE: Sodium Dodecyl Sulphate - Polyacrylamide Gel Electrophoresis

SER: Serine

SkM: Skeletal Muscle

SIRT1: Sirtuin 1

SIRT3: Sirtuin 3

SPA: Scintillation Proximity Assay

STZ: Streptozotocin

T

T1D: Type 1 Diabetes

T2D: Type 2 Diabetes

TGs: Triglycerides

TNF-a: Tumor Necrosis Factor alpha

TR: Thyroid Hormone Receptor

U

UCP1: Uncoupling Protein 1

UCP3: Uncoupling Protein 3

UV-B: Ultra-Violet B

W

WAT: White Adipose Tissue

WHO: World Health Organization

ABSTRACT

Background. Abscisic acid (ABA) is an isoprenoid hormone present in unicellular organisms and conserved across kingdoms in modern plants and animals. In mammals, ABA is produced by different cell types and is involved in tissue-specific physiological functions, such as inflammation, hemopoietic stem cell regeneration and control of blood glucose levels. The latter occurs through the insulin-independent stimulation of glucose uptake and metabolism in adipose tissue and skeletal muscle through its receptor LANCL2.

The aim of this study was to investigate whether:

- LANCL1, another member of the LANCL protein family, also behaves as an ABA receptor, sharing signalling pathway and functional properties with LANCL2 in the control of muscle glucose uptake;
- ABA could improve glycemic control in a murine model of (insulin-deficient) type 1 diabetes.

Methods. Rat L6 myoblasts overexpressing or silenced for LANCL1 and LANCL2, treated or not with ABA, were used to investigate the signalling pathway downstream of LANCL1 by Western Blot and qPCR experiments. Energy metabolism was studied in H9C2 cardiomyoblasts overexpressing or silenced for LANCL1/2 by monitoring the mitochondrial proton gradient. Finally, experiments were performed on LANCL2 knock-out mice, which overexpress LANCL1 in skeletal muscle, to investigate whether ABA could improve glucose tolerance after induction of insulin deficiency with streptozotocin.

Results. In L6 cells, both LANCL1 and LANCL2 mediate basal and ABA-stimulated glucose uptake (4-fold), activate transcription and protein expression of the glucose transporters GLUT4 and GLUT1 (4-6-fold) and the AMPK/PGC-1a/Sirt1 signalling proteins (2-fold).

In H9c2, overexpression of LANCL1 and LANCL2 increases, while their combined silencing almost abrogates, the mitochondrial proton

gradient. LANCL2 knock-out mice have a reduced glucose tolerance compared to WT, but they do respond to chronic ABA treatment (1 µg/kg BW/day) with an improved glycemia response to glucose load and an increased skeletal muscle transcription of GLUT4, GLUT1 (20-fold) and of the AMPK/PGC-1a/Sirt1 axis.

In mice rendered diabetic with low dose streptozotocin, chronic treatment with ABA improves glycemia control. In mice treated with high-dose streptozotocin (causing complete insulin deficiency) treatment with ABA improves the effect of low-dose insulin on glycemia control. In diabetic mice, ABA treatment increases skeletal muscle expression of the AMPK/PGC-1a/Sirt1 axis, of glucose transporters GLUT1/4, of the insulin receptor and of glycolytic enzymes.

Conclusions. Having regard to the results of this study, the conclusions are:

- LANCL1 shares with LANCL2 similar properties as an ABA receptor, stimulating glucose transport in skeletal muscle, mitochondrial function in cardiomyoblasts and whole-body glucose disposal.
- ABA supplementation in conjunction with insulin holds promise as a means to reduce the dose of insulin required for glycemia control, reducing the risk of hypoglycaemia, and improving skeletal muscle insulin sensitivity and glucose consumption as well as cardiomyocyte mitochondrial function.

INTRODUCTION

Abscisic acid (ABA)

2-Cis, 4-trans-abscisic acid is a naturally occurring isoprenoid hormone *(Magnone M. et al, 2015)* that was originally identified in plants in the 1960s *(Zocchi E. et al, 2017)*.

ABA has a chiral center, as indicated in Fig. 1, and the two enantiomers (R)-ABA and (S)-ABA both have a hormonal activity *(Lin B.L. et al, 2005)*. The natural enantiomeric form in plants is (S)-ABA.

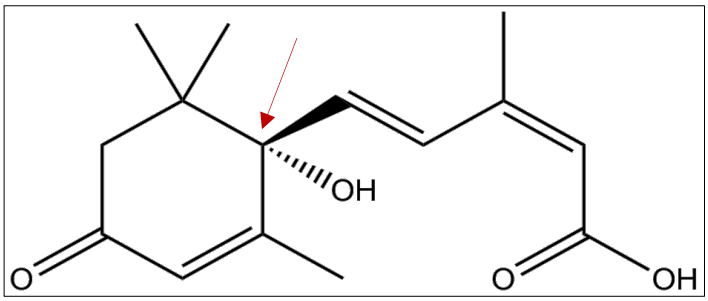

Figure 1. Chemical structure of Abscisic Acid.
The molecule is a 15-carbon weak acid (pKa 4,8), with an asymmetric carbon (indicated by the red arrow) which generates R-(-)-ABA and S-(+)-ABA.

Despite hormones are strictly specific to plants or animals, ABA is conserved through the species, suggesting a very early evolution before the separation of Metaphyta and Metazoa (from sponges up to mammals, humans included) *(Magnone M. et al, 2020)*.

Role and function of ABA in different species

Plants

ABA plays a key role in plant physiology, controlling different responses to environmental stress (like different water and nutrient availability, temperature variations, excess ultraviolet-B light) *(Magnone M. et al, 2020) (Zocchi E. et al, 2017)*, seed dormancy, germination, control of stomal closure, root elongation *(Hey S.J. et al, 2010) (Magnone M. et al, 2015)* and control of turgor levels.

ABA mediates these types of plant responses by activating a signalling pathway shown in Fig. 2: it involves its binding to the specific receptor complex (RCARs/PYR1/PYLs) and then the consequent inactivation and activation of type 2C protein phosphatases and kinases respectively, leading to ABA-dependent modifications in the metabolism and gene expression *(Gomez-Cadenas A. et al, 2015) (Raghavendra A.S. et al, 2010) (Zocchi E. et al, 2017)*.

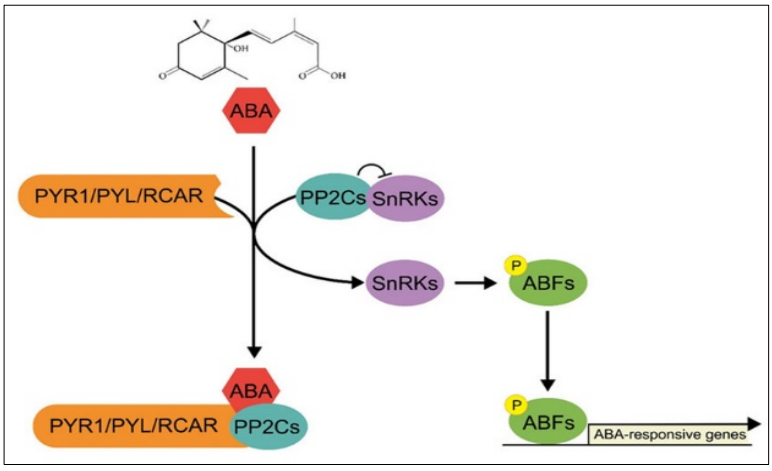

Figure 2. ABA signalling pathway in plants.
The ABA-signalling pathway initiates when the molecule is recognized by the complex PYR1/PYL/RCAR – PP2C – SnRKs. This complex formation activates the kinase SnRKs which in turn phosphorylates ABFs (transcription factors). ABFs binds the ABA-responsive genes *(Yoon Y. et al, 2020)*.

There are two known ABA biosynthesis pathways in plants, both resulting in the ABA precursor IPP (represented in Fig. 3):

- in chloroplasts, via the non-mevalonate biosynthesis pathway.
- In the cytosol, via the mevalonate biosynthesis pathway.

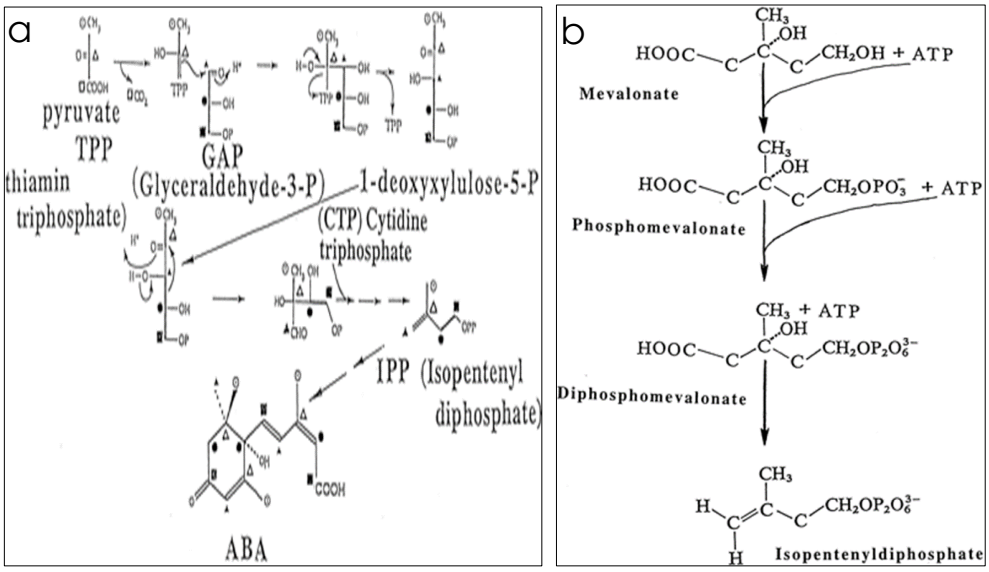

Figure 3. ABA biosynthesis pathway in plants.
IPP derives from Pyruvate and Glyceraldehyde-3-P in chloroplasts **(a)** and from mevalonate in cytosol **(b)**. *(Milborrow B.V., 2001)* (*Schwender et al, 1996)*; (*Kuzuyama et al, 1998)*; (*Rohdich et al., 1999)*.

Lower Metazoa

In organisms like sponges and hydroids, ABA controls the responses to the water temperature and light modifications: for example, in *Axinella polypoides* (a sponge, the oldest Metazoa), ABA is synthetized to respond to an increase of the water temperature, and it leads to water filtration and oxygen consumption *(Zocchi E. et al, 2017)*; in *Eudendrium racemosum* (a Hydroid, which shares with sponges a sessile lifestyle, and has a rudimental nervous system, digestive cavity and muscle and epithelial cells), endogenous ABA is synthetized under light stimulation, leading to stem cell-mediated tissue regeneration *(Zocchi E. et al, 2017)*.

Mammals (Humans)

The first detection in Mammals occurred in 1986, when it was found in pig and rat brains *(Le Page-Degivry M.T. et al, 1986)*, and its presence

was confirmed by HPLC-coupled mass spectrometry and biological activity. The study concluded that in mammals ABA derives both from the diet and is also produced endogenously.

In humans, the diet is crucial for ABA intake: there are some ABA-rich food sources, mostly fruit and vegetables that are listed in Fig. 4 *(Magnone M. et al, 2015)*. The dietary ABA is a GRAS (from FDA) ingredient, and it has some beneficial effects *in vivo* like reduced systolic blood pressure and aortic inflammation, increased insulin sensitivity and suppression of obesity-related inflammation in obese and diabetic cases *(Guri A.J. et al, 2007) (Guri A.J. et al, 2008) (Guri A.J. et al, 2010)*.

Fruits*—average total	0.62
Apple	0.30
Apricot	0.32
Avocado	2.0
Banana	0.22
Bilberry	0.4
Citrus	1.25
Fig	0.72
Pepper fruit	0.25
Persimmon	0.10
Vegetables*—average total	0.29
Barley	0.20
Cucumber	0.09
Maize	0.33
Pea	0.13
Potato	0.09
Soybean	0.79
Tomato	0.20
Wheat	0.15

Figure 4. Concentration of ABA in various foodstuff.
List of various ABA-rich food sources with content in mg/kg (mostly fruits and vegetables) *(Zocchi E. et al, 2017)*.

The endogenous production has been confirmed, even if the specific synthesis pathway has not yet been identified *(Zocchi E. et al, 2017)*: there is some evidence that ABA is produced in different types of human cells leading to autocrine or paracrine responses (tissue-specific physiological functions) *(Magnone M. et al, 2015)*.

- Innate immune cells → ABA was identified as a pro-inflammatory cytokine produced by human granulocytes, monocytes/macrophages, and microglia to stimulate these cells in an autocrine way in response to chemical and physical stimuli: basically, it works as a proinflammatory cytokine *(Bodrato N. et al, 2009) (Bruzzone S. et al, 2007) (Magnone M. et al, 2009)*. The result is an activation of mechanisms like phagocytosis, cell migration, production of NO and ROS (in granulocytes) *(Bruzzone S. et al, 2007) (Tossi V. et al, 2012)* and an autocrine stimulation of cytokine release, including TNFa and PGE_2. *(Magnone M. et al, 2009) (Magnone M. et al, 2012)*.
- Mesenchymal and hematopoietic stem cells → they release ABA, that in turn stimulates the production of growth factors responsible for cell proliferation *(Fresia C. et al, 2016) (Scarfì S. et al, 2008) (Scarfì S. et al, 2009)*.
- Keratinocytes → the absence of ABA receptor causes the inhibition of the inflammatory response induced by UV-B *(Tossi V. et al, 2012)*. Thus, ABA positively influences inflammatory mechanisms like ROS and NO production, PGE_2 and TNFa release induced by UV-B.
- Adipocytes → ABA treatment induces a lower triglyceride accumulation, CO_2 production, synthesis of fatty acids from glucose, increase of mitochondrial content, enhanced O_2 consumption and increase of the transcription of adiponectin and of brown adipose tissue (BAT)-specific genes *(Sturla L. et al, 2017)*.
- Skeletal muscle cells → they respond to ABA with an increased glucose transport mediated by the translocation of the GLUT4 transporter on the plasma membrane *(Bruzzone S. et al, 2012)*.
- β-pancreatic cells → high glucose levels stimulate these cells to release ABA, which in turn stimulates insulin secretion from the same cells both in a glucose-independent and glucose-dependent manner (for example, ABA concentration in the

human plasma increases after a glucose overload, so it means that ABA is produced in response to the increase of glycemia) *(Bruzzone S. et al, 2008) (Bruzzone S. et al, 2012) (Magnone M. et al, 2015)*.

The ABA/LANCL system

Receptors

The mammalian ABA receptors belong to the conserved lanthionine synthetase C-like (LANCL) protein family *(Fresia C. et al, 2016)*.
These enzymes are the homologues of the prokaryotic lanthionine synthetase component C (LANC) protein, a cyclase involved in the modification of lanthionine and peptides *(Bauer H. et al, 2000) (Cichero E. et al, 2018)*: this zinc-containing enzyme catalyses the production of lantibiotics (as represented in Fig. 5), that have antimicrobial properties *(Sahl H.G. et al, 1998)*.

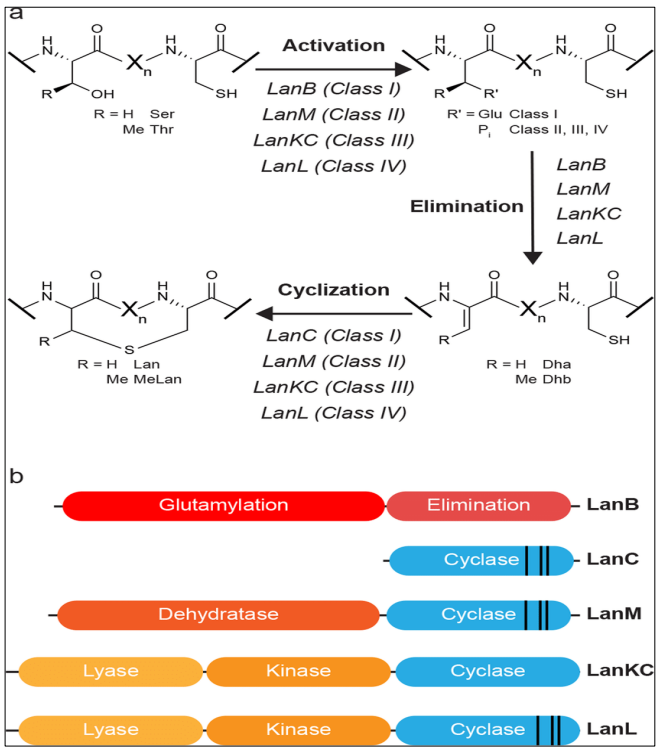

Figure 5. Biosynthesis of lanthipeptides.
LanC enzymes catalyse the addition of the Cys thiol to the dehydrated Serine *(Walker M.C. et al, 2020)*.

Although the name "lanthionine synthetase" protein family recalls this prokaryotic origin, none of the mammalian LANCL proteins synthetizes lanthionine: the triple knock-out (KO) of LANCL1, LANCL2 and LANCL3 does not reduce the levels of brain lanthionine ketimine (a lanthionine metabolite) *(He C. et al, 2017)*.

This evidence suggests that LANCL proteins must have a different function in Mammals.

The human genome encodes three distinct LANCL protein: LANCL1, LANCL2 and LANCL3, located on chromosomes 2, 7 and X, respectively *(Katoh M. et al, 2003) (Mayer H. et al, 2001)*. The RNA and protein expression profiles are shown in Fig. 6 and 7.

- LANCL1 was isolated from human erythrocyte membranes in 1998 as the first member of this family *(Mayer H. et al, 1998)*. This protein is localized both in the cytosol and in the nucleus.
- LANCL2 was isolated after LANCL1 in skeletal muscles, immune cells, heart, placenta, lung, pancreas, liver, prostate, and central nervous system *(Mayer H. et al, 2001)*. The protein is ubiquitary, but the highest levels are observed in the brain. *(Spinelli S. et al, 2021)*.

  LANCL2 is bound to the intracellular side of the plasma membrane through the myristoylated N-terminal Gly residue *(Cichero E. et al, 2018) (Landlinger C. et al, 2006)*. It can activate a G-protein and then translocate to the nucleus (when demyristoylated), like a steroid hormone receptor *(Fresia C. et al, 2016)*.

  The fact that LANCL2 is not a transmembrane protein has been proved *in silico* and *in vitro* with different experiments like chemical treatments and inhibition of the myristoylation: mutation on Gly2 prevents the myristoylation and abrogates the ABA signalling pathway *(Fresia C. et al, 2016)*.
- LANCL3 appears to be a pseudogene and it is expressed at a very low level in human cells *(Sturla L. et al, 2009) (Cichero E. et al, 2018)*.

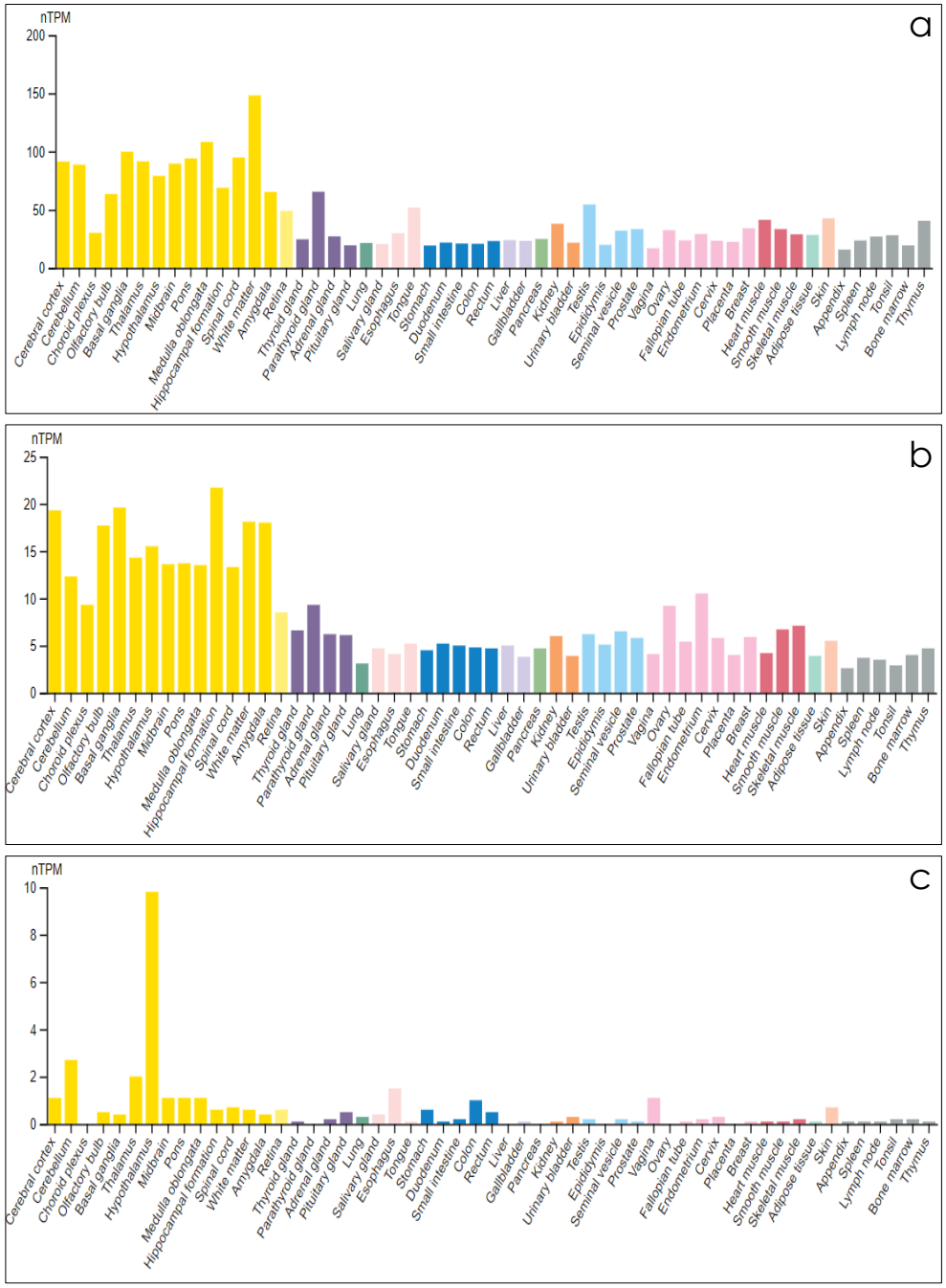

Figure 6. LANCL1, LANCL2 and LANCL3 RNA expression profiles in human tissues. Overview of the RNA expression of the three receptors LANCL1 **(a)**, LANCL2 **(b)** and LANCL3 **(c)** in different tissues from different organs *(The Protein Atlas)*.

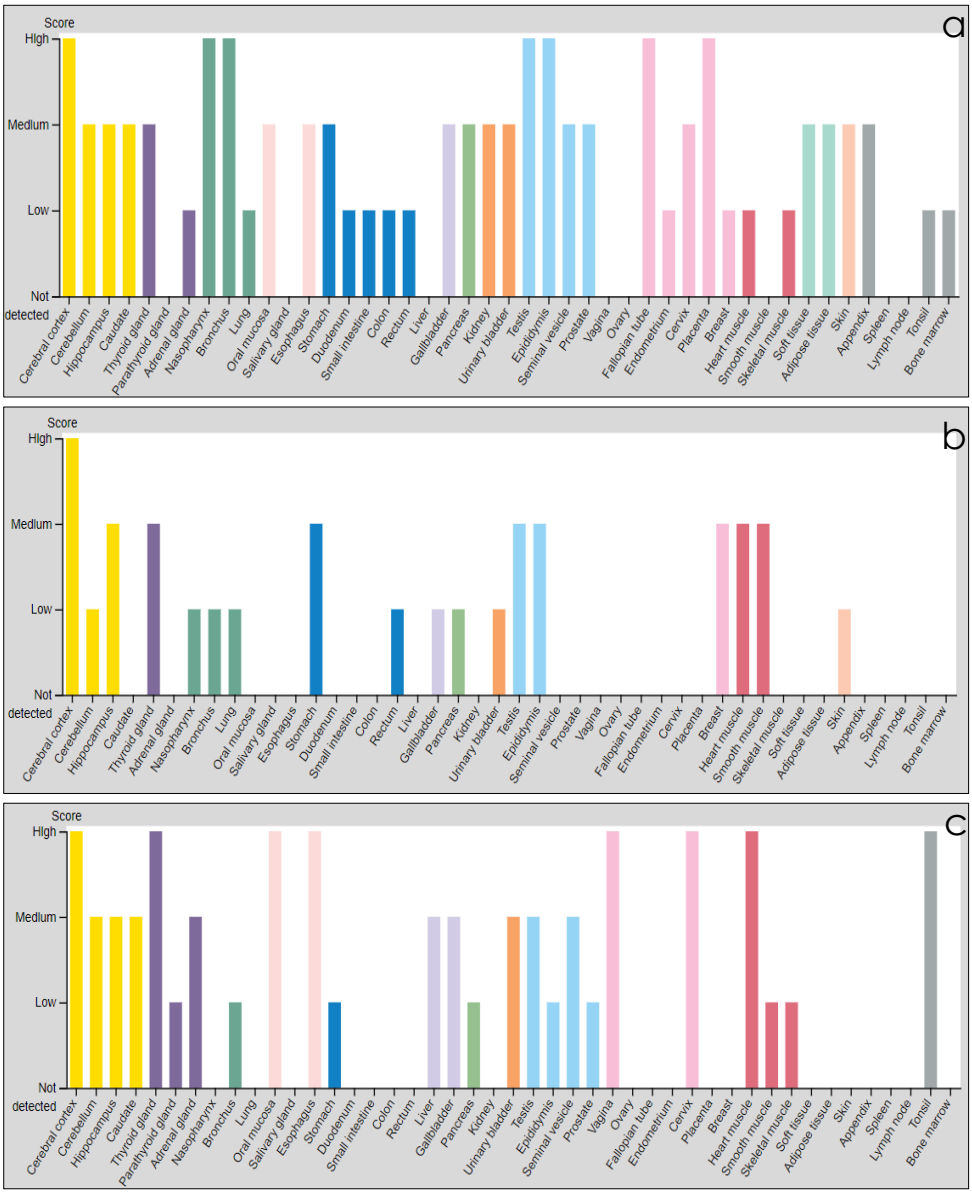

Figure 7. LANCL1, LANCL2 and LANCL3 protein expression profiles in human tissues.
Overview of the protein expression of the three receptors LANCL1 **(a)**, LANCL2 **(b)** and LANCL3 **(c)** in different tissues from different organs *(The Protein Atlas)*.

Both LANCL1 and LANCL2 were originally described as GPCR receptors (called GPCR69A and GPCR69B) and they share a high sequence homology (more than 70%) *(Fresia C. et al, 2016) (Landlinger C. et al, 2006)*. The reason for hypothesizing a role for the mammalian LANCL proteins as putative ABA receptors was their homology with a plant

GPCR (GCR2), originally proposed as an ABA receptor *(Liu X. et al, 2007)*.

Several in vitro techniques indicate that human recombinant LANCL2 indeed binds ABA with a high affinity (Kd 2,6 nM) *(Cichero E. et al, 2018) (Sturla L. et al, 2011)*. Two different recombinant proteins were used (LANCL2-GST and LANCL2 cleaved from its GST tag) and different methods to assess ABA binding were employed, including (R, S)-[3H] ABA, scintillation proximity assay (SPA), dot blot and affinity chromatography.

The ABA signalling pathway

The ABA signalling pathway was described for the first time in granulocytes (Fig. 8) *(Bruzzone S. et al, 2007)*.

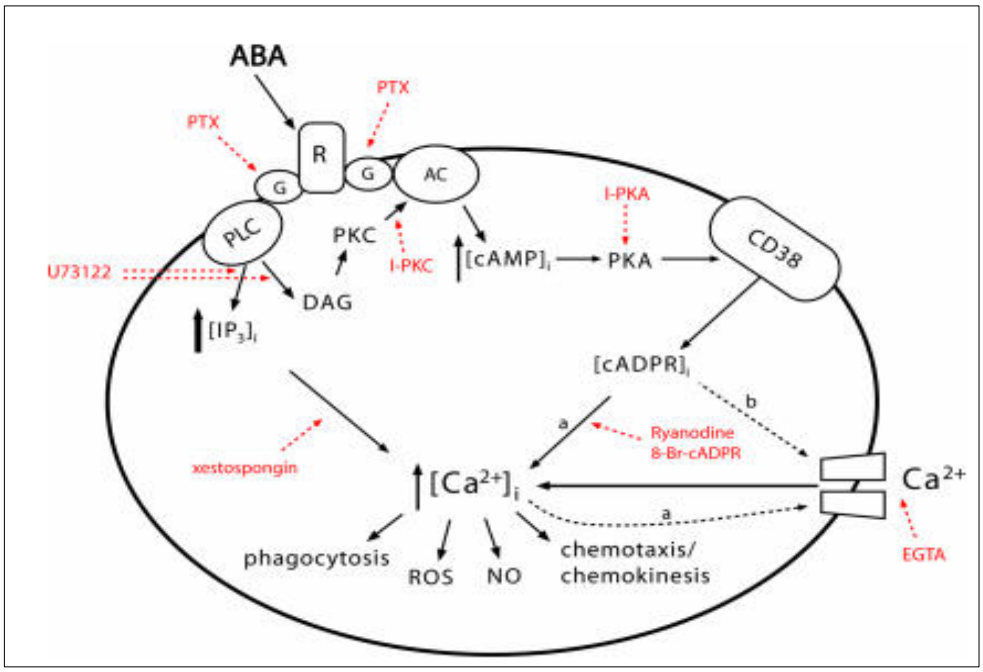

Figure 8. ABA signalling pathway in granulocytes.
Mechanism of the ABA-induced $[Ca^{2+}]_i$ increase mediated by a GPCR, activation of both PLC and adenylate cyclase, eventually leading to an intracellular Ca^{2+} increase. Site-specific inhibitors of the ABA-signalling pathway are indicated in red *(Bruzzone S. et al, 2007)*.

Further studies in other mammalian cell types (keratinocytes, hemopoietic progenitors, mesenchymal stem cells, insulin-releasing pancreatic cells) confirmed a similar ABA signalling pathway and

demonstrated the essential role of LANCL2 as the ABA receptor *(Bruzzone S. et al, 2008)*.

ABA, binding to LANCL2, triggers the activation of a Pertussis (PTX)-sensitive G protein, leading to the sequential activation of AC (with overproduction of cAMP), PKA and to the phosphorylation and activation of the ADP-ribosyl cyclase CD38 which converts NAD^+ to cADPR. This leads to an increase of both extracellular Ca^{2+} entry and (CICR)-mediated intracellular Ca^{2+} mobilization *(Lee H.C. et al, 1989) (Wu Y. et al, 1997)*. Activation of the G protein also induces the activation of PLC, which produces another Ca^{2+}-mobilizing second messenger, IP3, concurring to the eventual Ca^{2+}-induced Ca^{2+} influx from the plasmatic membrane. The ABA/LANCL2 system, when the binding occurs, translocates into the nucleus *(Fresia C. et al., 2016)*: this behaviour is typical of peptide and steroids receptors. The increase of intracellular free Ca^{2+} concentration in turn activates several cell-specific functions in granulocytes, such as a rapid extravasation and consequent cell migration (chemotaxis, chemokinesis), phagocytosis, and the release of reactive oxygen species and nitric oxide *(Bruzzone S. et al, 2007)*.

Conservation of this signalling pathway from lower Metazoa to Humans, maybe suggests that this pathway is evolutionarily conserved through the species, and it is essential *(Zocchi E. et al, 2017)*.

In hematopoietic progenitors, the overproduction of cAMP leads to the activation of CREB *(Scarfì S. et al, 2009)*.

Besides, other evidence demonstrates that LANCL2, after the binding with ABA, is able to directly interact with Akt and, consequently, phosphorylate it (independently from the insulin pathway) *(Zeng M. et al, 2014)*.

LANCL2 facilitates Akt phosphorylation through mTORC2, which is known to phosphorylate Akt on Ser-473 *(Alessi D.R. et al, 1997) (Sarbassov D.D. et al, 2005)*, leading to increased GLUT4 expression and plasma membrane translocation. These results allow to hypothesize a role for ABA via LANCL2 in the control of muscle glucose

uptake (GLUT4 is indeed predominantly expressed in the skeletal muscle) and of glycemia (Fig. 9).

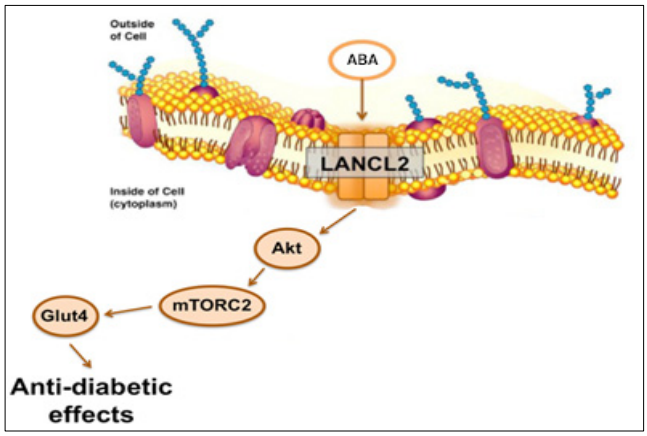

Figure 9. Hypothetical role of ABA signalling pathway through LANCL2 involving mTORC2.
In muscle, ABA can activate Akt and consequently mTORC2 by phosphorylation, through LANCL2 receptor; the result is glucose uptake through GLUT4 and glycemia control. *(Alessi D.R. et al, 1997) (Sarbassov D.D. et al, 2005)*

Role of the ABA/LANCL2 system in adipocytes

Adipose tissue is one of the largest tissues present in human body: it has a fundamental role in the control of glycemia, in the control of glucose and lipid concentration, and in energy balance *(Sturla L. et al, 2017)*.

There are two types of adipose tissue (AT): white (WAT), specialized in the production of triglycerides (TGs) to store the energy, and brown (BAT), which is responsible for energy expenditure *(Cannon B. et al, 2004) (Cinti S., 2002)*.

For the first time, it has been demonstrated that:

- AT can release ABA in response to high glucose levels *(Bruzzone S. et al, 2012)*.
- ABA stimulates adipocyte glucose uptake by increasing GLUT4 translocation to the plasma membrane *(Bruzzone S. et al, 2012)*
- In vivo, ABA stimulates BAT glucose uptake and transcription of browning genes in the BAT and in the WAT from ABA-treated mice *(Sturla L. et al, 2007)*.

- LANCL2 is also involved in some activities typical of adipocytes: on the one hand, ABA via LANCL2 stimulates the transcription of "browning" genes in white adipocytes; on the other hand, ABA via LANCL2 stimulates mitochondrial biogenesis and respiration in brown adipocytes and increases transcription of uncoupling proteins in the BAT from ABA-treated mice *(Sturla L. et al, 2017)*.

Role of the ABA/LANCL2 system in skeletal muscle

Recent results indicate that ABA stimulates uptake of the fluorescent glucose analog 2-NBDG by the rat myoblast cell line L6, and of [18F]-deoxy-glucose (FDG) by mouse skeletal muscle, with an insulin-independent mechanism *(Magnone M. et al, 2020)*.

Both effects rely on the activation by ABA of AMPK, as they are abrogated by the specific AMPK inhibitor dorsomorphin. In L6 cells, incubation with ABA increases phosphorylation of AMPK and upregulates the expression of PGC-1a, a master regulator of energy expenditure and mitochondrial function.

A causal role of LANCL2 in these ABA-mediated effects is demonstrated by their significant reduction after LANCL2 silencing.

In addition, low-dose oral ABA stimulates glucose uptake and storage in the skeletal muscle of rats undergoing an oral glucose load, as detected by micro-PET.

These results clearly indicate a role for the ABA/LANCL2 system in the control of muscle glucose uptake and metabolism, with an insulin-independent, AMPK-mediated mechanism.

Thus, it could be anticipated that LANCL2 knock-out (KO) mice would show a reduced glucose tolerance *(Magnone M. et al, 2020)*.

AIMS OF THE PROJECT

Based on the above-described experimental evidence, a role for the ABA/LANCL2 system emerges in the control of the expression of GLUT4 (particularly in skeletal muscle and in adipocytes), in the control of mitochondrial respiration (particularly in the adipose tissue) and in the insulin-independent stimulation of glucose uptake in skeletal muscle (SkM). In line with this conclusion, LANCL2 KO mice indeed show a reduced glucose tolerance.

However, unexpectedly, LANCL2 KO mice respond to ABA treatment with a significant reduction of the glycemia profile, after glucose load *(Magnone M. et al, 2020)*, suggesting the existence of another ABA receptor. This observation indicates the presence of (an)other ABA receptor(s) in addition to LANCL2 and the most likely candidate is LANCL1, because of the significant sequence identity (54.2%), similar intracellular localization (LANCL1 is a peripheral membrane protein) and tissue expression pattern of LANCL2 and LANCL1. Intriguingly, LANCL1 is indeed spontaneously overexpressed in the skeletal muscle of LANCL2 KO mice.

Thus, we undertook to study the possible role of LANCL1 as a second ABA receptor in the skeletal muscle, in addition to LANCL2, and more generally, the function of the ABA-LANCL hormone-receptor system in muscle physiology.

Specifically, the aim of this study was to test the hypothesis that, based on the insulin-independent stimulation by ABA of muscle GLUT4 expression and plasma membrane translocation, treatment with ABA could improve glycemic control in a murine model of insulin-dependent (type 1) diabetes (T1D).

We aimed to establish whether:

- exogenous ABA could reduce hyperglycemia in multiple low-dose streptozotocin STZ-treated mice (i.e., in the presence of markedly reduced endogenous insulin)

- ABA could improve the effect of suboptimal doses of insulin in single high-dose STZ-treated mice (i.e., in the absence of endogenous insulin).

In addition, since LANCL1 is overexpressed in the SkM of LANCL2 KO mice and activates the AMPK/PGC-1a/Sirt1 axis similarly to LANCL2 *(Spinelli S. et al, 2021)*, we compared the effect of ABA on STZ-treated LANCL2 KO and LANCL2+/+ (wild-type) mice, to verify whether LANCL1 could substitute for LANCL2 in mediating the effect of ABA on the skeletal muscle in diabetic mice.

In addition, we investigated the effect of the overexpression or of the silencing of LANCL1 and LANCL2 on the mitochondrial proton gradient of the murine cardiomyoblast cell line H9c2.

MATERIALS AND METHODS

Cloning of LANCL1 and LANCL2 in pBABE Vector

The full-length of hLANCL1 was amplified from 1 ng of the LANCL1-pGEX-6-P1 *(Sturla L. et al, 2009)* vector by PCR using the following primers:

- 50-ATT**GGATCC**ATGGCTCAAAGGGCCTTCCCG-30 (forward-BamHI restriction site underlined) for the cloning in the pBABE vector (Addgene, MA, USA)
- 50-AAT**GAATTC**TCAGAGTTCAAATGCAGGGAACC-30 (reverse-EcoRI restriction site underlined) for the cloning in the pBABE vector (Addgene, MA, USA).

The full-length of hLANCL2 was amplified from 1 ng of the LANCL2-pGEX-6-P1 vector *(Sturla L. et al, 2009)* by PCR using the following primers:

- 50-ATT**GAATTC**ATGGGCGAGACCATGTCAAAGAG-30 (forward-EcoRI restriction site underlined) for the cloning in the pBABE vector (Addgene, MA, USA).
- 50-AAT**GTCGAC**TTAATCCCTCTTCGAAGAGTCAAG-30 (reverse-XhoI restriction site underlined) for the cloning in the pBABE vector (Addgene, MA, USA).

The PCR was performed in 25 µl containing 1X reaction buffer, 300 µM dNTP, 7.5 pmol of primers, and 2.5 units of Pfx50™ DNA Polymerase (Thermo Fisher Scientific, Milan, Italy).

The PCR reaction profile was 1 cycle at 94 °C for 2 min, 35 cycles at 94°C for 15 s, 60°C for 30s, and 68°C for 1 min with a final extension for 5 min at 68°C.

The PCR products were purified from agarose gel with a QIAEX II Gel Extraction Kit (Qiagen, Milan, Italy), digested with the restriction enzymes and cloned into pBABE using a Rapid Ligation Kit (Roche, Milan, Italy).

The two vectors were purified using Plasmid Mini Kit (Qiagen, Milan, Italy) sequenced by TibMolbiol (Genoa, Italy) and used to transform E. Coli BL21 (Agilent Technologies, Milan, Italy).
The recombinant proteins produced by bacteria are human LANCL1 and human LANCL2 fused with GST; after purification, the GST is cleaved by PreScission Protease to obtain the final purified hLANCL1 and hLANCL2 proteins.

Cell Culture

In this work, we used 4 different cell lines:

- HEK-293T cell line is an epithelial-like cell line isolated from the kidney tumour of a patient, and it was purchased from ATCC (ATCC CRL-3216).
  HEK-Platinum-A (Plat-A) cell line were developed from HEK293T cell line and was provided by Cell Biolabs (RV-102). They contain *gag*, *pol* and *env* genes (necessary to allow retroviral packaging and the production of high yield of retroviruses).
- L6 cell line (ATCC CRL-1458) is a myoblast cell line obtained from rat skeletal muscle.
- H9c2 cell line (ATCC CRL-1446) is a subclone of the original cell line obtained from embryonic rat heart tissue.

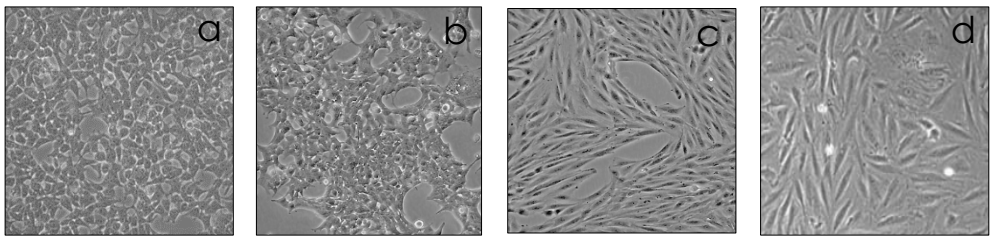

Figure 10. Images of cell lines from ATCC.
Morphology of HEK-293T **(a)**, HEK PLAT-A **(b)**, L6 **(c)** and H9c2 cells **(d)** observed at the microscope.

All cell lines (represented in Fig. 10) were cultured in DMEM containing 10% FBS, 100 IU/ml penicillin and 100 µg/ml streptomycin and maintained in a humidified 5% CO_2 atmosphere at 37°C.

Lentiviral and Retroviral Cell Transduction

Overexpression of human LANCL1 (ovLANCL1) and human LANCL2 (ovLANCL2) in L6 and H9c2 cells was obtained using pBABE vectors constructed as described before, together with the empty vector pBABE (Addgene) as negative control.

The following protocol was used:

1,5 x10^4 HEK Plat-A cells were seeded in 6 cm Petri dishes and transfected when they were 60-70% confluent. Cells were cotransfected with 4 µg of plasmids and 200 ng of pCMV-GFP *(Cea M. et al, 2016)* using TransIT® Transfection Reagent (Mirus, Madison, USA).

The day after, the medium was changed to remove the non-transfected DNA from the HEK Plat-A; meanwhile, 5 x10^5 cells were seeded in 10 cm Petri dishes to start the transduction.

We performed 2 infections/day for two days to collect the supernatant containing lentiviral particles: the supernatant was filtered with a 0,45-µm-diameter filter and used to infect L6 and H9c2 cells in the presence of protamine sulfate (5 µg/ml the first in the morning and the second in the late afternoon). After these four transductions, we selected with puromycin (5 µg/ml) the cells which have internalized the plasmids.

The overexpression efficiency was evaluated by Real Time PCR and Western Blot (mRNA and protein levels).

For the silencing, we used other lentiviral plasmids like pLV[shRNA]-Puro-U6 encoding for the scramble control and for the shRNA targeting rat LANCL1 and LANCL2 (plasmid ID: VB010000-0005mme – VB181016-1107sen – VB181016-1124zjp) purchased from Vector Builder (Chicago, IL, USA); moreover, we replace HEK Plat-A with HEK-293T cells using the same procedure described before.

Real time PCR

L6 cells, seeded in a 6-wells plate, were incubated with or without 100 nM ABA for 4 and 24 hours.

Besides, quadriceps muscles were taken, after sacrifice, from mice chronically treated with or without ABA for 4 weeks (1 µg/kg BW/day)
Total RNA was extracted on the one hand from L6 cells using RNeasy Micro Kit (Qiagen, Milan, Italy), according to the manufacturer's instructions, and on the other hand from muscle using QIAzol Lysis Reagent and Tissue Lyser Instrument (Qiagen, Milan, Italy).
The cDNA was synthesized by using iScript cDNA Synthesis Kit (Bio-Rad) starting from 1 µg of total RNA and was used as a template for qPCR analysis: reactions were performed in an iQ5 Real-Time PCR detection system (Bio-Rad) *(Sturla L. et al, 2009)*. The mouse and rat specific primers were designed using Beacon Designer 2.0 software (Bio-Rad), and their sequences are listed below.
The qPCR amplification reaction was performed in triplicate and had a volume of 25 µl, containing: the primer mixture (0,4 µM of sense and antisense primer), 12,5 µl of 2X iQ SYBR Green Supermix Sample (Bio-Rad, Milan, Italy) and 4 ng of cDNA.
The amplification program is composed by 40 cycles of two steps, the heating at 95°C and 62°C and the fluorescence was detected at the end of each cycle.
Statistical analysis of the qPCR was performed using the iQ5 Optical System Software version 1.0 (Bio-Rad Laboratories) based on the 2_ΔΔCt method *(Livak J. et al, 2001)*. The dissociation curve for each amplification was examined to confirm the absence of nonspecific PCR products.

Mouse Genes	Accession N°	Forward Primer	Reverse Primer
Actb	NM_007393	GCGAGAAGATGACCCAGATC	GGATAGCACAGCCTGGATAG
Gapdh	GU214026	CGTGCCGCCTGGAGAAACCTG	TGGAAGAGTGGGAGTTGCTGTTGAAG
Hprt1	NM_013556	CCCTGGTTAAGCATACAGCCCC	AGTCTGGCCTGTATCCAACACTTCG
Ins	NM_008386 NM_001185083	GTGAAGTGGAGGACCCACAA	GCTGGTAGAGGGAGCAGATG
Lancl1	NM_001190985	GAGGGCCTTTCCGAATCCTT	GGAGTCAGCCTCCCAGTAGA
Lancl2	NM_133737	GCCTCCCTTTCCACCCTAACG	GTCCGTCGTCTTCAGTCCTTCC
Nampt	NM_021524	AATGTCTCCTTCGGTTCTGGTG	CCCGCTGGTGTCCTATGTAAAG
Ppargc1a	NM_008904	CCCTGCCATTGTTAAGACC	TGCTGCTGTTCCTGTTTTC
Pdha1	NM_008810	GATGGAGCTAAAGGCGGATCA	TCCGTAGGGTTTATGCCAGC
Pfkm	NM_001163487	AGTTGGTATCTTCACGGGCG	CATAGACACGCTCTCCCACG
Prkaa1	NM_001013367	AGAAGCAGAAGCACGACGG	TTGCCCACCTTCACTTTCCC
Sirt1	NM_019812	GCAGGTTGCAGGAATCCAAAGGA	GGGCACCGAGGAACTACCTGA
Slc2a1	NM_011400	GCCCATCCCATCCACCACACTC	CCATAAGCACAGCAGCCACAAAGG
Slc2a4	NM_009204	CCAGCCTACGCCACCATAG	TTCCAGCAGCAGCAGAGC
Rat Genes	**Accession N°**	**Forward Primer**	**Reverse Primer**
Actb	NM_031144	GGGAAATCGTGCGTGACATT	GCGGCAGTGGCCATCTC
Hprt1	NM_012583	TTGGTCAAGCAGTACAGCCC	TGGCCTGTATCCAACACTTCG
Lancl1	NM_053723	TCTTGCTCCTCATCCTGCTCATC	CACTGTACTCGCCGAAGGTCTC
Lancl2	NM_001014187	GGTGCCACGGTGCTCCAG	CCTCGCTGCCAAATCACATCAC
Ppargc1a	NM_031347	GCACACATCGCAATTCTCCC	CTCTGCGGTATTCGTCCCTC
Prkaa1	NM_019142	AGAAGCAGAAGCACGACGG	GAAGGTGCCGACGCCC
Sirt1	NM_001372090	CAGTGTCATGGTTCCTTTGC	CACCGAGGAACTACCTGAT
Slc2a1	NM_138827	GACCCTGCACCTCATTGGT	CTCAGATAGGACATCCAGGGC
Slc2a4	NM_012751	CCAGCCTACCGCCACCATAG	TTCCAGCAGCAGCAGAGC

Table 1. Mouse and Rat primers.
List of Mouse and Rat primers, with forward and reverse sequences, used for Real Time PCR.

Western blot

Western blot experiments were performed both on L6 cells (seeded in 6 cm Petri using complete DMEM and then incubated with or without 100 nM ABA for 1 and 24 hours) and quadriceps muscles isolated from wild type LANCL2 KO mice (treated or not with 100 nM ABA).
After that, samples were processed for Western blot experiments.

After removal of the supernatant and washing with PBS, cells were scraped in 300 µl of lysis buffer (20 mM TrisHCl pH 7.4, 150 mM NaCl, 1 mM EDTA, 1% NP40) containing a protease inhibitor cocktail (PIC).
After brief sonication and a centrifugation for 10 minutes at 12.000 RCF, the protein concentration was determined on an aliquot of each lysate with Bradford Assay.
For the quadriceps, the same procedure was followed with the only difference that these tissues were lysed with the Tissue Lyser (Qiagen, Milan, Italy) and centrifuged without sonication.
Lysates (70 µg proteins from tissues and 40 µg proteins from cells) were loaded on 10% polyacrylamide gel and separated by SDS-PAGE. Proteins were transferred to nitrocellulose membranes (Bio-Rad), according to standard procedures.
The membranes were blocked for 1 h with PBST (137 mM NaCl, 2.7 mM KCl, 1.8 mM KH_2PO_4, 10 mM Na_2HPO_4, 1% Tween) containing 5% non-fat dry milk, and incubated overnight at 4°C with primary antibodies (listed below).
Following incubation with the appropriate secondary antibodies (listed below) and ECL detection (GE Healthcare), band intensity was quantified with the ChemiDoc imaging system (Bio-Rad).

Primary Antibody	**Host**	**Concentration**	**Manufacturer**
Anti-βActin	Mouse	1:1000	Santa Cruz Biotechnology Inc., California
Anti-AMPK	Rabbit	1:1000	Cell Signaling Technology, Danvers, MA
Anti-GLUT4	Mouse	1:200	Cell Signaling Technology, Danvers, MA
Anti-LANCL1	Rabbit	1:250	Novus Biologicals
Anti-LANCL2	Mouse	1:1000	*(Vigliarolo T. et al, 2015)*
Anti-p-AMPK (Ser473)	Rabbit	1:1000	Cell Signaling Technology, Danvers, MA
Anti-Pgc1a	Mouse	1:1000	Sigma Aldrich
Anti-Vinculin	Rabbit	1:1000	Cell Signaling Technology, Danvers, MA
Secondary Antibody	**Concentration**		**Manufacturer**
Anti-Mouse	1:2000		Santa Cruz Biotechnology Inc., California
Anti-Rabbit	1:1000		Santa Cruz Biotechnology Inc., California

Table 2. Primary and Secondary Antibodies.
List of Primary and Secondary antibodies used for Western Blot.

Glucose transport assay

L6 cells silenced or overexpressed for LANCL1 and LANCL2, together with their respective control, were seeded with a density of 1 x 10^4 cells/well in a 96 multiwell (each experimental condition was performed in at least 8 wells) and cultured overnight using 5 mM DMEM without serum. After that, cells were washed once with DMEM and then incubated for 5 minutes at 37° C in DMEM with 100 nM ABA or 2 mM metformin. After the incubation, cells were washed with KRH at 37° C and 50 µM 2-NBDG (a fluorescent deoxyglucose analogue) was added to each well. After 10 minutes, the supernatant was removed, cells were washed with ice-cold KRH and 50 µl of KRH was added to each cell. The mean fluorescence (l_{ex} = 465 nm / l_{em} = 540 nm) was calculated from 10 acquisitions/well. Unspecific 2-NBDG uptake, determined in the presence of the glucose transport inhibitors cytochalasin B (20 mM) and phloretin (200 mM), was subtracted from each experimental value *(Magnone M. et al, 2020)*.

JC-1 staining and analysis

H9c2 cells were stained with the cationic dye JC-1 (Thermo Fisher Scientific, Waltham, MA), which exhibits potential-dependent accumulation in mitochondria.

At low membrane potentials, JC-1 exists as a monomer and produces a green fluorescence (emission at 527 nm), whereas at high membrane potentials JC-1 forms aggregates and produces a red fluorescence (emission at 590 nm).

Thus, mitochondrial depolarization is indicated by a decrease in the red/green fluorescence intensity ratio *(Chen G. et al, 2018)*. Briefly, H9c2 cells were seeded at 3x10^4 onto µ-slide wells, stained with JC-1 (2,5 µg/ml) for 20 min at 37°C in a 5% CO_2 incubator and then imaged live. The red/green ratio was analysed after a background subtraction with the ImageJ software (v1.8.0, National Institutes of Health, Bethesda, MD, USA), using a quantitative analysis based on an intensity measurement of specific selected ROIs.

Animals

All mice used in the experiments belong to C57BL/6 strain (obtained from Charles River, Milano, Italy) and were housed at the IRCCS San Martino Hospital (Genoa, Italy) animal facility. All protocols of animal use were approved by the Italian Ministry of Health, in line with the EU Directive 2010/63/EU for animal experiments.

First, heterozygous animals were derived from KO females backcrossed with WT males *(Magnone M. et al, 2020)*.

The homozygous mice used in this work were derived from a heterozygous breeding scheme (LANCL2 +/- x LANCL2 +/-). The genotype was validated before starting with the experiments.

In vivo experiments

Experiment 1

Seven-week-old mice (9/group) were fed a standard diet, and they were administered ABA (Merck) 1µg/kg BW for 4 weeks in the drinking water, following a protocol published in a previous work *(Magnone M. et al, 2020)*. To calculate the ABA concentration in drinking water, a preliminary study was performed, in which the daily volume of water consumed, and the average weight of mice were determined (animals were weighed weekly).

Experiment 2

For this study, only male mice were used, because females are less susceptible to diabetes induction with STZ *(Zamboni F. et al, 2021) (King A.J.F. et al, 2020)*.

STZ (Cayman Chemical, Michigan, USA) solution was prepared immediately before use in sterile saline water and injected i.p. with two different protocols:

- Multiple low dose treatment was performed with STZ 20 mg/kg BW/day for 5 consecutive days. The result is a progressively increase of the glycemia profile over several weeks: it allows us

to test the effect of chronic ABA in the presence of residual endogenous insulin.

- Single high-dose treatment was performed with STZ 200 mg/kg BW. The result is a rapid development of hyperglycaemia (>500 mg/dL) over few days: this protocol allowed to test the effect of ABA in a condition of complete insulin deficiency.

For all the tests eight-week-old mice were used, fed a normal diet. To study the effect of ABA (5 µg/kg BW either chronically administered or taken as a single dose), the molecule was administered in the drinking water or as a single dose by gavage, respectively.

Oral Glucose Tolerance Test (OGTT)

Experiment 1

Mice were fed for 4 weeks a standard diet enriched with ABA or not (control), and one week before the end of the diet they were fasted for 17 hours: after that, 1g/kg BW glucose was administered by gavage in 150 µl of water. Blood was collected from the tail vein before gavage (time 0) and 15, 30, 60 and 120 min after gavage: glycemia was immediately measured in duplicate with a glucometer (Ascensia, Milan, Italy).

Experiment 2

Mice were fasted for 6 hours before the OGTT. Given that the basal glycemia is increased due to the STZ treatment, the dose of glucose was reduced from the usual 1g/kg BW to 0,25 g/kg BW administered in 150 µl of water by gavage with or without 5 µg/kg BW of ABA.
The blood, collected from the tail vein before gavage (time 0) and 15, 30 60 and 130 min after gavage, was analysed and glycemia was measured in duplicate with a glucometer (Ascensia, Milan, Italy).
The absolute AUC was calculated with the trapezoidal rule from the values of glycemia (mg/dL), while the incremental AUC was calculated from the glycemia values relative to time 0.

Plasma ABA, insulin determination and ex vivo analysis of murine skeletal muscle

Experiment 1

One week after the OGTT, animals were sacrificed, and samples of plasma were used to determine ABA concentration (ELISA kit Agdia). Besides, quadriceps muscles were taken and flash frozen in liquid nitrogen for Western blot analysis and mRNA extraction.

Experiment 2

Insulin (Toujeo, Sanofi Aventis, Paris, France) was injected subcutaneously (after having diluted it just before the use in a mildly acidic aqueous solution). ABA was administered by gavage immediately prior to insulin (at the concentration of 5 µg/kg BW) while control mice received an equal amount of water by gavage. Plasma, taken from the tail vein or from the orbital sinus, were centrifuged and frozen immediately in dry ice. Blood samples were used to measure the insulin concentration with an ELISA kit (ultrasensitive insulin ELISA, Mercodia, Winston Salem, NC, USA).

Statistical analysis

Continuous variables are presented as mean ± SD. Comparisons were drawn by an unpaired, two-tailed Student's t-test, if not otherwise indicated.
Statistical significance was set at $P < 0.05$.

RESULTS

Silencing and overexpression of LANCL1 and LANCL2 in L6 rat myoblasts

In previous studies, we showed that ABA, via LANCL2, is able to stimulate glucose transport in muscle cells via an insulin-independent increase of GLUT4 expression *(Magnone M. et al, 2020)*: now we wanted to investigate if LANCL1 could have a similar role in the same function. For this purpose, we prepared both the stable silencing and the overexpression of rLANCL1 and rLANCL2 in rat L6 myoblasts.

With a lentiviral infection, using shRNAs, and a subsequent puromycin selection of the infected cells, we obtained the stable knockdown of both LANCL1 and LANCL2, confirmed by both qPCR (Fig. 11, central panel) and immunoblot (Fig. 11, right panel).

With a retroviral infection, we obtained the overexpression of LANCL1 and LANCL2, confirmed by immunoblot (Fig. 11, left panel).

All the experiments were performed with a silencing efficiency of approx. 80% for both LANCL1 and LANCL2 compared with control cells (infected with a scramble shRNA) and an overexpression of approx. 4-fold for LANCL1 and 6-fold for LANCL2 relative to control cells (infected with an empty vector PLV).

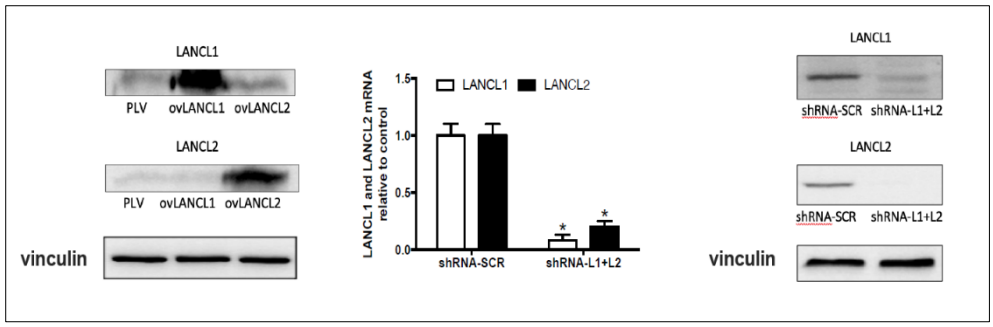

Figure 11. Validation of overexpression and silencing for LANCL1 and LANCL2 in L6 rat myoblasts cell line.
Representative Western Blot of the overexpression of LANCL1 (ovLANCL1) and LANCL2 (ovLANCL2) protein **(left panel)**. Representative Western Blot of the silencing for both proteins together (shRNA-L1+L2) **(right panel)**. mRNA levels of LANCL1 and LANCL2 in silenced cells relative to control **(central panel)**.
*p < 0.0002 by unpaired two-tailed t-test.
The data are the mean ± SD from 3 different determinations.

Silencing or overexpression of ABA receptors in L6 cells affects glucose transport via GLUT4 and the expression of AMPK, PGC-1a, SIRT1 and GLUT1/4

In silenced L6 cells infected with the empty vector (PLV), ABA stimulated NBDG uptake approx. 2-fold compared to untreated controls.

Overexpression of either LANCL1 or LANCL2 increased the effect of ABA on NBDG uptake (Fig. 12, left panel), also increasing the effect of metformin, a known stimulator of cell glucose uptake via GLUT4 *(Lee J.O. et al, 2011)*.

Conversely, LANCL1 and LANCL2 silencing showed the opposite effect, abrogating the effect of ABA on NBDG uptake and significantly reducing the effect of metformin (Fig. 12, right panel).

As metformin is a known activator of AMPK, we may conclude that the ABA-LANCL system and metformin share the same effector kinase AMPK.

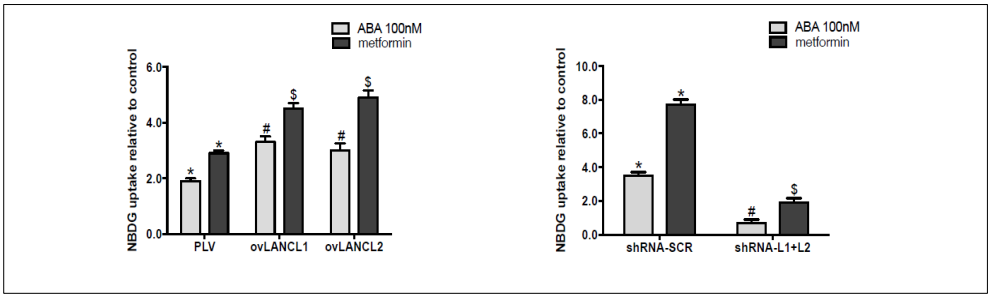

Figure 12. NBDG uptake in overexpressing and silenced cells.
L6 cells overexpressing and silenced for LANCL1 and LANCL2 were starved for 12 hours and then treated with 100 nM ABA or 2 mM metformin for 5 minutes before the incubation with NBDG. NBDG uptake in overexpressing **(left panel)** and silenced cells **(right panel)** respectively related to untreated control cells.
*p < 0.0004 relative to untreated PLV; #p < 0.001 relative to ABA-treated PLV; $p < 0.0002 relative to metformin treated PLV for left panel. *p < 0.0004 relative to untreated scramble cells; #p < 0.00007 relative to ABA-treated scramble cells; $p < 0.0001 relative to metformin-treated scramble cells.
All the experiments are the mean ± SD from at least 3 separate experiments.

Indeed, the stimulation of glucose transport by ABA via LANCL2 occurs via the activation of AMPK and increased transcription of PGC-1a *(Magnone M. et al, 2020)*. In LANCL2-overexpressing cells, we observed an increased transcription of AMPK, PGC-1a, Sirtuin 1 (Sirt1)

and GLUT4, all key molecular players in muscle function and metabolism *(Petrocelli J.J. et al, 2020)* (Fig. 13).

Interestingly, GLUT1-specific mRNA was also more abundant in LANCL2-overexpressing cells. Treatment with 100 nM ABA for 4 hours further increased the transcription of all the above proteins (Fig. 13).

A similar pattern of results was observed on LANCL1-overexpressing cells, indicating that AMPK, PGC-1a, Sirt1, GLUT4, and GLUT1 are also targets of LANCL1 (Fig. 13).

Interestingly, the overexpression of either LANCL1 or LANCL2 increased the transcription of AMPK, GLUT4, GLUT1, PGC-1a and Sirt1 even in the absence of added ABA.

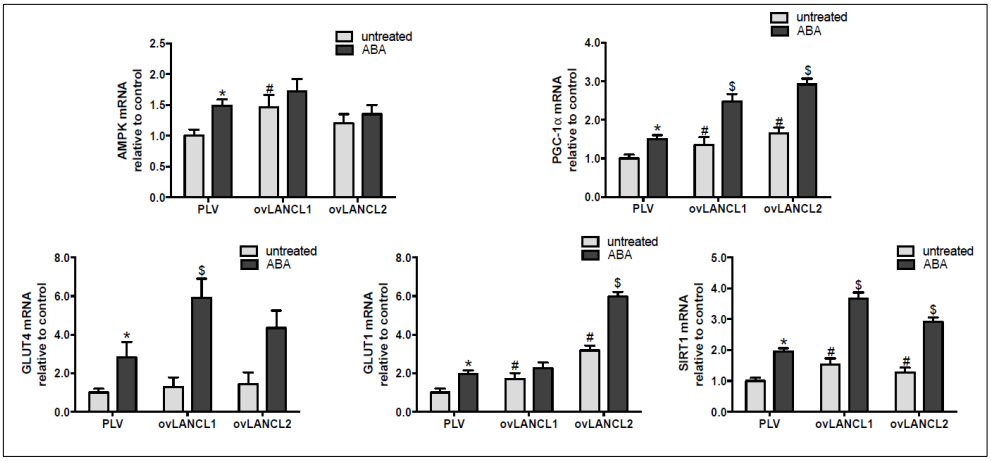

Figure 13. mRNA transcription levels of GLUT4/1 and AMPK/PGC-1a/SIRT1 axis.
L6 cells were starved for 12 hours, then treated with 100 nM ABA for 4 hours. mRNA levels of the indicated proteins are expressed relative to untreated PLV control cells.
*p < 0.02 relative to untreated control cells; #p < 0.05 and $p < 0.05 relative to untreated controls. $p < 0.01 and #p < 0.02 relative to ABA-treated control.
P values are calculated by unpaired two-tailed t-test.
Results are the mean ± SD of 3 separate experiments.

Next, we investigated whether LANCL1/2 silencing had an effect on the transcription of the same regulatory proteins.

The combined silencing of LANCL1 and LANCL2 significantly reduced the basal (unstimulated) level of mRNAs for all the target proteins and GLUT4 compared to scramble control cells (Fig. 14).

Upon incubation with 100 nM ABA for 4 hours, the levels of all mRNAs explored increased in LANCL1/2-silenced cells, except for the GLUT4

mRNA, though they remained below those measured in untreated, scramble control cells (Fig. 14).

The partial abrogation of the response to ABA may be attributed to the incomplete knockdown of LANCL1/2 expression accomplished by shRNA infection (approx. 80%).

Taken together, these observations indicate a transcriptional control exerted by the LANCL1/2 proteins on the genes explored (AMPK, PGC-1a, Sirt1, and GLUT4).

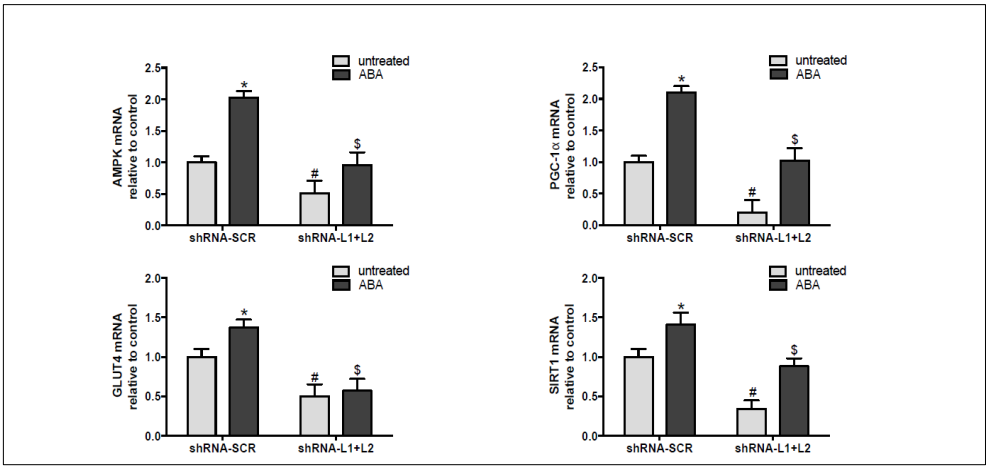

Figure 14. mRNA transcription levels of GLUT4 and AMPK/PGC-1a/SIRT1 axis.
L6 cells were starved for 12 hours, then treated with 100 nM ABA for 4 hours. mRNA levels of the indicated proteins are expressed relative to scramble control cells. *p < 0.02 relative to untreated control cells; #p < 0.05 and §p < 0.05 relative to untreated controls. $p < 0.01 and §p < 0.02 relative to ABA-treated control.
P values are calculated by unpaired two-tailed t-test.
Results are the mean ± SD of 3 separate experiments.

At the protein level, total AMPK increased slightly in L6 cells overexpressing LANCL2, but not LANCL1; upon treatment with ABA, both AMPK (Fig. 15, upper left panel) and p-AMPK (Fig. 15, upper right panel) significantly increased in cells overexpressing either LANCL1 or LANCL2, indicating that both LANCL1 and LANCL2 stimulate AMPK protein expression and phosphorylation upon ABA binding. A higher amount of the total and phosphorylated AMPK increases the enzymatic activity of the kinase, both potential and actual, on its different substrates. Thus, although the p-AMPK/AMPK ratio was similar in control and in LANCL1/2-overexpressing cells incubated with ABA, the significantly higher total amounts of p-AMPK and total AMPK in the

overexpressing cells implies a higher kinase activity. We observed a 2-fold increase of PGC-1a, GLUT1, and GLUT4 protein expression in LANCL1/2-overexpressing L6 cells and treatment with ABA further increased these protein levels in a similar way in both overexpressing L6 cell lines. (Fig. 15, lower panel). Thus, protein expression increased in parallel with mRNA transcription.

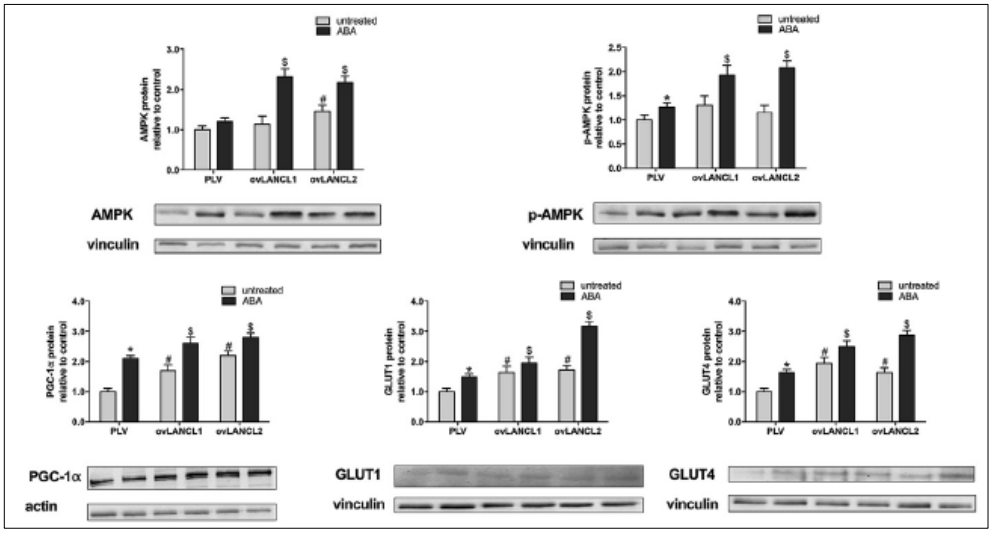

Figure 15. Protein expression levels of GLUT4/1 and AMPK/PGC-1a axis in overexpressing cells.
L6 myoblasts were serum-starved for 12 hours and then incubated with or without 100 nM ABA for 1 hour and then the protein levels were analysed with Western Blot. AMPK, p-AMPK (Ser473) **(upper panels)**, PGC-1a, GLUT1 and GLUT4 **(lower panels)** relative to PLV control cells.
*p < 0.03 and #p < 0.006 relative to untreated control; $p < 0.02 relative to ABA-treated PLV control cells.
P values are calculated by unpaired two-tailed t-test.
Each panel shows the mean ± SD of at least 3 different experiments and a representative Western Blot of the investigated protein.

On the contrary, the double-silenced cells showed a significant reduction of total and phosphorylated AMPK, which increased slightly upon ABA treatment of the cells, but remained lower than protein levels in the control cells, infected with scramble-shRNAs (Fig. 16, upper right and left panels). PGC- 1a, GLUT1 and GLUT4 protein levels were lower in double-silenced cells as compared to the control cells and remained below the levels of control cells upon treatment with ABA (Fig. 16, lower panel).

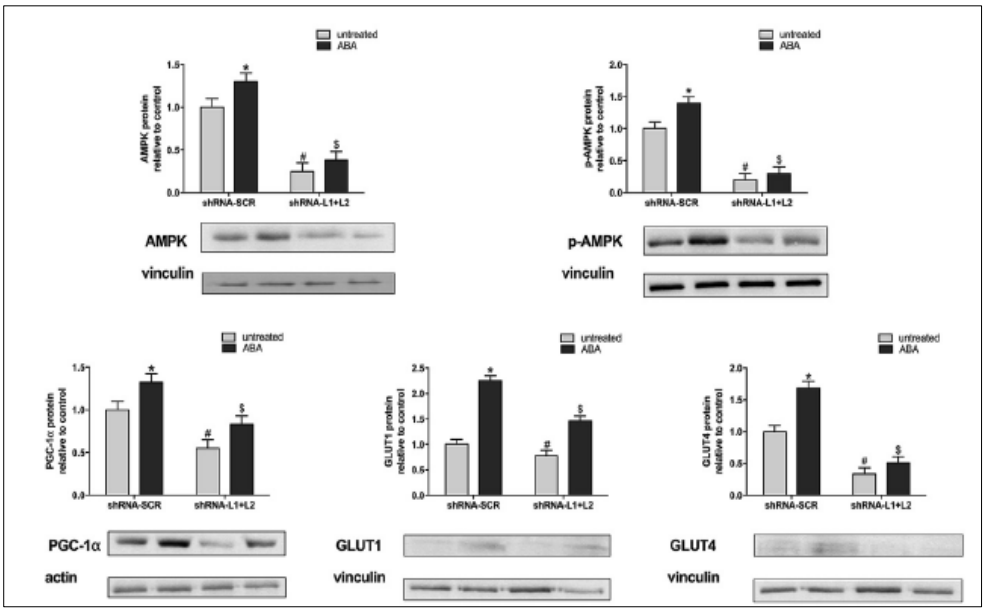

Figure 16. Protein expression levels of GLUT4/1 and AMPK/PGC-1α axis in silenced cells.
L6 myoblasts were serum-starved for 12 hours and then incubated with or without 100 nM ABA for 1 hour and then the protein levels were analysed by Western Blot. AMPK, p-AMPK (Ser473) **(upper panels)**, PGC-1a, GLUT1 and GLUT4 **(lower panels)** relative to scramble control cells.
*p < 0.02 and #p < 0.01 relative to untreated control; $p < 0.008 relative to ABA-treated scramble control cells.
P values are calculated by unpaired two-tailed t-test.
Each panel shows the mean ± SD of at least 3 different experiments and a representative Western Blot of the investigated protein.

Finally, we observed that ABA treatment significantly increased the expression of both glucose transporters GLUT4 and GLUT1 in the plasma membrane-enriched fractions of overexpressing cells compared with control cells (Fig. 17).

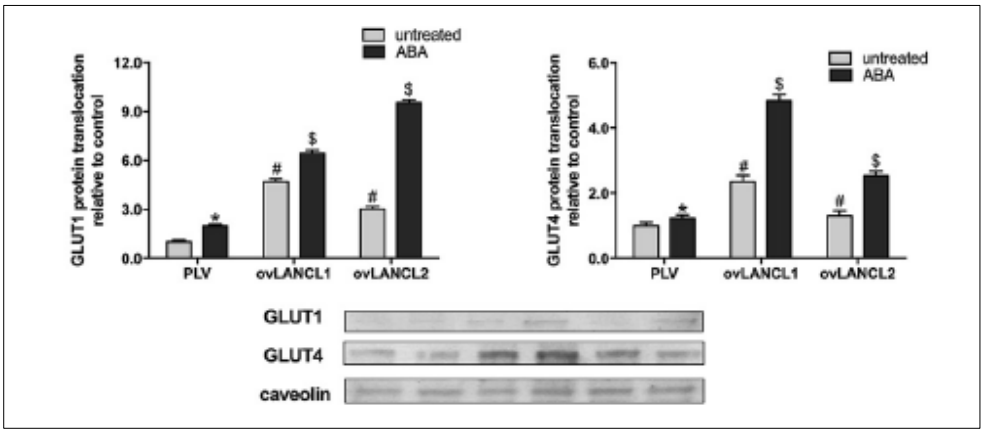

Figure 17. GLUT1/4 protein translocation in overexpressing cells.
Plasma membrane-enriched lysates from L6 overexpressing cells treated or not with ABA were obtained (see Materials and methods section). GLUT1 and GLUT4 protein expression relative to PLV control cells.
*p < 0.04 and #p < 0.008 relative to untreated control; $p < 0.03 relative to ABA-treated PLV control cells.
P values are calculated by unpaired two-tailed t-test.
Each panel shows the mean ± SD of at least 3 different experiments and a representative Western Blot of the investigated protein.

ABA improves glucose tolerance *in vivo* via LANCL1/2 by stimulating GLUT4 expression in muscle cells via the AMPK/PGC-1a axis

LANCL2 KO mice show a significantly reduced glucose tolerance *(Magnone M. et al, 2020)* and we confirmed this result by comparing the glycemia profile of wild-type (WT) (LANCL2+/+) and LANCL2 -/- (KO) mice after an oral glucose load (Fig. 18, left panel). In the time frame between 0 and 30 min, glycemia increased significantly faster in KO than in WT mice. When both groups of mice were treated with chronic ABA (1 µg/kg BW/day for 4 weeks), a significant reduction of the area-under-the-curve (AUC) of glycemia was observed. (Fig. 18, right panel)
It follows that the absence of LANCL2 did not abrogate sensitivity to the glycemia-lowering action of ABA.

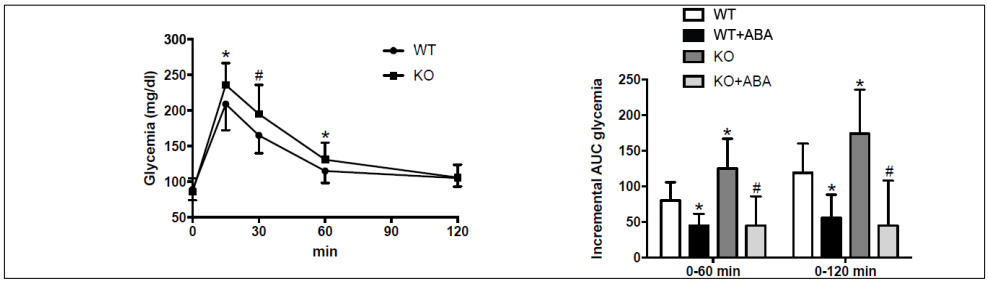

Figure 18. Glycemia profile and relative AUC in WT and KO mice.
7-week-old LANCL2 KO mice (KO) and their wild-type siblings, 9 per group, were subjected to an oral glucose tolerance test (OGTT). Glycemia profile monitored by tail vein puncture at the indicated time points after gavage **(left panel)**.
*p < 0.04 and #p < 0.01 relative to WT.
Incremental AUC of glycemia **(right panel)** calculated, in the indicated time frames, with the trapezoidal rule on the glycemia increase relative to time zero in WT and KO mice undergoing an OGTT with or without ABA at 1 mg/kg BW, in addition to glucose.
*p < 0.05 relative to WT; #p < 0.003 relative to KO.

The next step was to analyse the expression levels of LANCL1 in the skeletal muscle (quadriceps) from LANCL2 KO and WT mice.
LANCL1 expression in LANCL2 KO mice was significantly higher if compared with control mice; interestingly, both LANCL1 mRNA and protein expression further increased after chronic treatment of mice with oral ABA (Fig. 19).

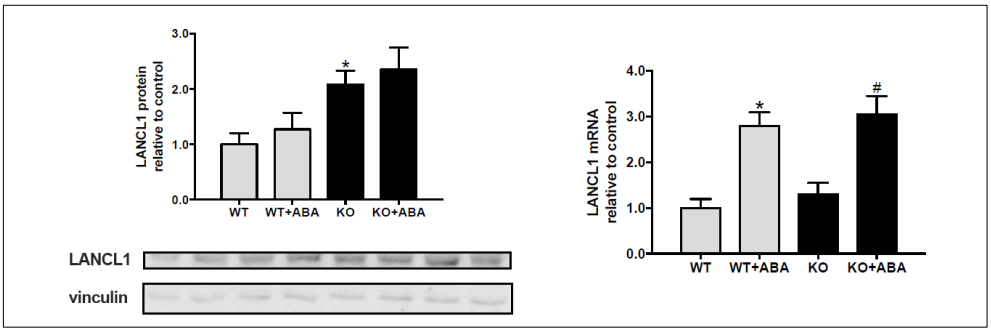

Figure 19: LANCL1 expression of both protein and mRNA in skeletal muscle samples from WT and KO mice.
A representative Western blot analysis and Real Time PCR are shown for 2 animals for each condition. *p < 0.05 relative to WT; #p < 0.02 relative to KO; $p < 0.05 relative to ABA-treated WT.
P values are calculated by unpaired two-tailed t-test.

Thus, we investigated the mRNA levels of AMPK, PGC-1a, GLUT4, GLUT1 and also of Sirt1and of NAMPT, both being targets of PGC-1a. Transcription of all these proteins was significantly higher in the ABA-treated mice (both LANCL2 KO and WT) compared with the respective untreated controls (Fig. 20); given that the increase was similar in WT and LANCL2 KO mice, we can conclude that the absence of LANCL2 does not affect the stimulatory effect of oral ABA on the transcription of these proteins.
We already know that the overexpression of NAMPT controls and maintains mitochondrial NAD^+ levels *(Yu A. et al, 2020)*, enhancing exercise endurance in mice *(Costford S.R. et al, 2018)*.
Indeed, chronic ABA treatment significantly increased physical performance and endurance in mice *(Costford S.R. et al, 2018) (Magnone M. et al, 2020)*. KO mice showed higher protein levels of PGC-1a and GLUT4 than WT controls, which did not further increase upon ABA treatment (excluding AMPK) and were similar to those of

WT mice treated with ABA (Fig. 20, left panel). The ratio between p-AMPK and AMPK in ABA treated and untreated mice, both WT and KO, was similar and approximately 1 (not shown), in line with what observed in L6 cells overexpressing LANCL1 or LANCL2.

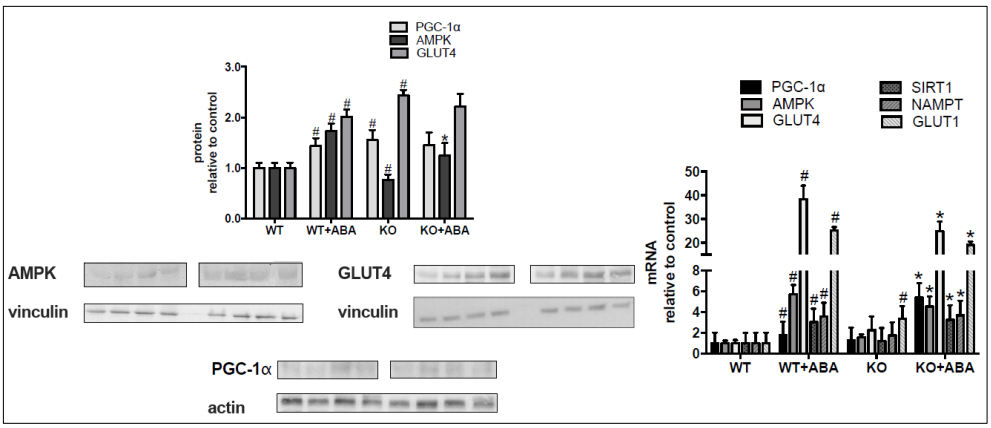

Figure 20. Protein and RNA expression of GLUT1/4, AMPK/PGC-1α/SIRT1 axis and NAMPT in WT and KO mice.
Expression of AMPK, PGC-1a, GLUT4 protein **(left panels)** and GLUT1/4, AMPK, PGC-1a, SIRT1, NAMPT mRNA **(right panel),** expressed relative to levels in untreated WT muscle.
#p < 0.05 relative to WT; *p < 0.04 relative to KO.
P values are calculated by unpaired two-tailed t-test.
A representative Western blot analysis is shown for 2 animals for each condition.

Altogether, the results described above and obtained on myoblasts over-expressing or silenced for LANCL1/2 and on LANCL2 KO mice allow to conclude that both LANCL proteins share a common signaling pathway, involving AMPK and PGC-1a, which activates glucose transport in muscle cells in vitro and in vivo.

The fact that this signaling pathway occurs via AMPK makes it different from that of insulin, which instead activates Akt, leading to the same functional effect, i.e. increased glucose transport and metabolism.

The insulin-independent nature of the ABA/LANCL system is also confirmed by previous observations, where glucose transport was stimulated in murine muscle biopsies treated with ABA ex vivo, i.e. in the absence of insulin *(Magnone M. et al, 2020)*.

These results prompted us to hypothesize that, by activating muscle glucose uptake via an insulin-independent mechanism, ABA could

ameliorate glucose tolerance in conditions were insulin secretion is impaired, such as in T1D.

Chronic Low-Dose ABA Improves Glycemia in Mice Rendered Diabetic with Multiple-Low Dose STZ

The aim of multiple low-dose STZ injections (20 mg/Kg BW/day for 5 days) protocol was to obtain a progressively increasing glycemia in treated mice: in our experience, mice reached glycemia values of approximately 400 mg/dL one month after treatment with this protocol of diabetes induction.

In our protocol, we decided to divide LANCL2+/+ (WT) mice into two groups, one of which was treated with ABA at a dose of 5 µg/Kg BW, administered in the drinking water. Starting at day 4, and for 5 consecutive days (until day 9), both groups of mice were injected i.p. with STZ at a dose of 20 mg/Kg BW/day.

A significant reduction in glycemia was observed in the ABA-treated group as compared with ABA-untreated controls, starting from day 14. Glycemia increased during the period when the animals were monitored: the peak was 395 ± 64 mg/dL and 294 ± 69 mg/dL at day 28 in the control and ABA-treated groups, respectively ($p = 0.029$) (Fig. 21).

At day 30, an OGTT was performed with glucose 0.25 g/Kg BW administered by gavage and glycemia was monitored for 90 min. the glycemia was decreased in the ABA-treated compared with control mice (Fig. 21, upper panel), with a significant reduction in the AUC of glycemia in the time frame analysed (Fig. 21, lower panel).

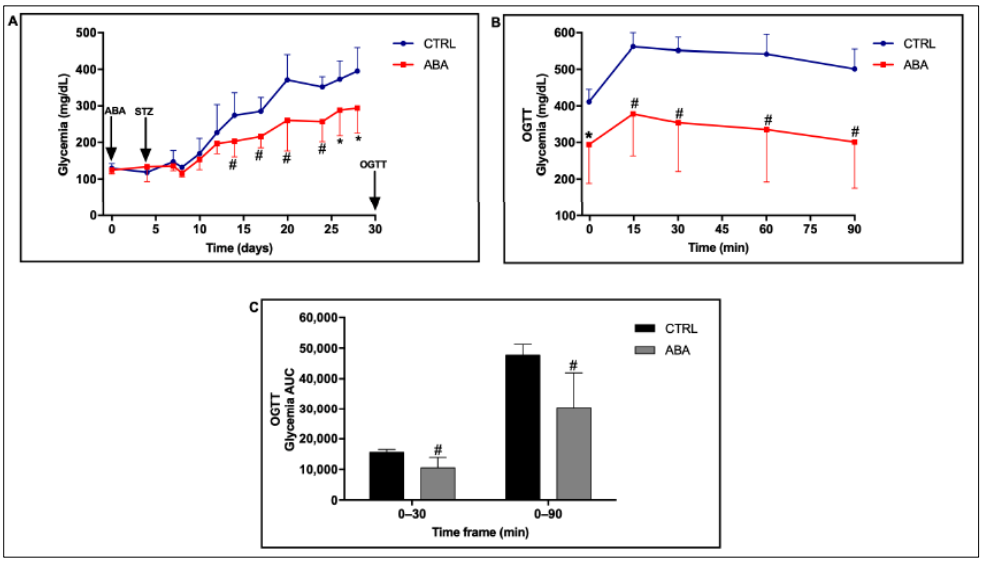

Figure 21. Glycemia profile during the treatment and after the OGTT (together with the respective AUC) in WT mice.
Eight-week-old LANCL2 WT mice divided into two groups (8 mice/group) and treated or not (CTRL) with ABA 5µg/kg BW/day before diabetes induction with multiple low dose STZ (20 mg/kg BW/day) for 5 days. Glycemia profile over 30 days and ABA treatment starting at day 0 and followed by STZ treatment at day 4 **(A - upper left panel)**. Glycemia profile during OGTT performed at day 30 with glucose 0,25 g/kg BW with or without ABA **(B - upper right panel)**. AUC of the glycemia profile of the OGTT **(C - lower panel)**.
*p < 0.05, #p < 0.02, relative to CTRL.
P values are calculated by unpaired two-tailed t-test.

Besides, we decided to investigate the effect of chronic ABA treatment, started after the onset of hyperglycaemia: for this purpose, we applied the same protocol as before, starting however with ABA treatment (5 µg/Kg BW/day) at day 8 when mean glycemia was ≥ 250 mg/dL in both animal groups (Fig. 22). The result didn't change in the ABA-treated mice, the glycemia profile was again significantly lower compared with the controls, starting from 5 days after onset of chronic ABA treatment (day 13).

At day 30, after treatment with ABA for 22 days, the effect of low-dose insulin on glycemia was explored by means of the s.c. injection of 0.1 U of insulin (4 mU/g BW) (Fig. 22, upper panel). A significant reduction in the glycemia profile after insulin administration was observed in the ABA-treated mice as compared with ABA-untreated mice (Fig. 22, upper panel), with a significant 50% reduction in the AUC of glycemia in the timeframe 120–240 min (Fig. 22, lower panel).

Four days after the insulin test, the animals were euthanized and we performed RT-PCR analysis on SkM from the two mice groups: the analysis revealed a significant increase in the transcription of AMPK (6-fold), PGC-1a (2-fold), and GLUT4 (40-fold) in ABA-treated mice as compared with ABA-untreated mice (Fig. 22, lower panel).

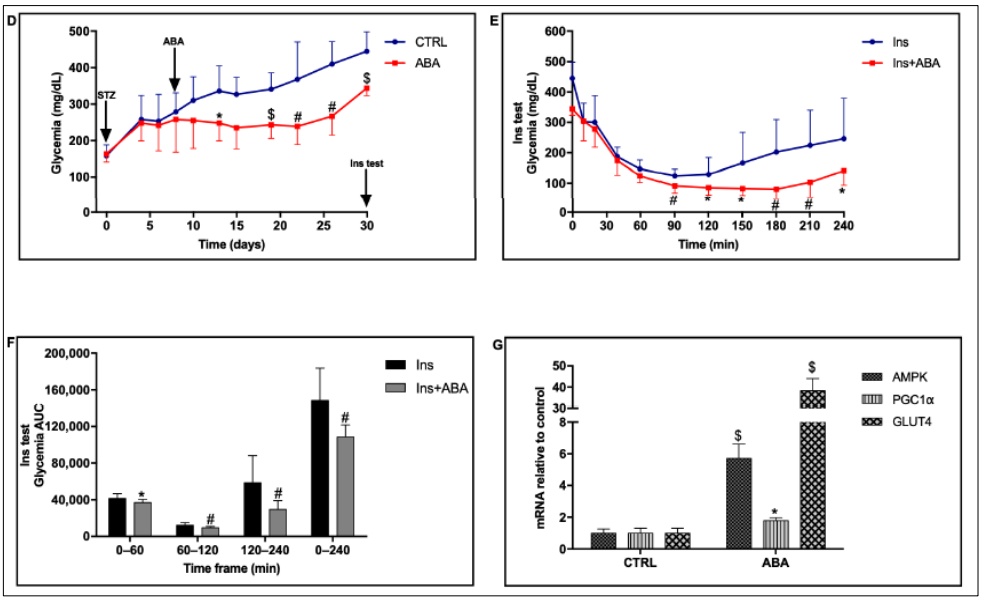

Figure 22. Glycemia profile during ABA and insulin treatment (together with relative AUC) and mRNA expression for AMPK, PGC-1a and GLUT4.
Eight-week-old LANCL2 WT mice divided into two groups (8 mice/group) were treated or not (CTRL) with ABA 5 µg/kg BW/day after diabetes induction with multiple low dose STZ (20 mg/kg BW/day) for 5 days. Glycemia profile over 30 days, ABA treatment starting 3 days after the STZ treatment **(D - upper left panel)**. Glycemia profile of the insulin test performed at day 30 with 0.1 U of insulin injected at time 0 **(E - upper right panel)**. AUC of the glycemia profile of the insulin test **(F - lower left panel)**. mRNA expression of AMPK, PGC-1a and GLUT4 in the skeletal muscle from mice sacrificed 4 days after the insulin test **(G - lower right panel)**.
*p < 0.05, #p < 0.02, $p < 0.005 relative to CTRL or insulin.
P values are calculated by unpaired two-tailed t-test.

Altogether, results shown in Fig. 22 indicate that oral ABA, administered either before or after onset of hyperglycaemia in a multiple low-dose STZ protocol, improved the glycemia profile, the response to a glucose load, and the effect of low-dose insulin. When administered after induction of diabetes with low-dose STZ, ABA ameliorated the efficacy of residual endogenous insulin on glycemia, resulting in a significantly reduced glycemia profile in the treated

animals (Fig. 22), and also improved the response to exogenous low-dose insulin (Fig. 22).

The increased transcription of the AMPK/PGC-1a signalling axis and of GLUT4 in the SkM from ABA-treated mice, compared with untreated controls, confirms previous observations *(Spinelli S. et al, 2021)* and could be part of the mechanism through which ABA improves glycemia. The increased expression of GLUT4 could also improve the efficacy of residual endogenous insulin on muscle glucose uptake.

A Single Oral Dose of ABA Improves the Efficacy of Insulin in Overtly Diabetic Mice

The next step was to assess if a single oral dose of ABA could improve the effect of insulin on hyperglycaemic mice. For this purpose, we applied a single-high-dose STZ protocol, which consists in a single administration of 200 mg/Kg BW STZ.

Previous results obtained in humans demonstrated that intake of a single dose of ABA, taken together with a meal, reduced the glycemia profile for up to 6 hours, indicating a long-lasting effect of oral ABA *(Magnone M. et al, 2015)*.

In the first part of the experiment, when glycemia was approx. 300 mg/dL in all animals, we administered s.c. 0.1 U insulin (4 mU/g BW) with or without oral ABA (5 µg/Kg BW). We analysed the results at different time frames during the development of hyperglycaemia.

The glycemia profile monitored over 4 h was significantly reduced in the ABA-treated animals as compared with controls, with a significant reduction in the AUC of glycemia, particularly in the timeframe 60–240 min (Fig. 23, upper right panel).

In the second part of the experiment, the insulin test (Fig. 23, lower panel), was performed with the same parameters when glycemia was ≥500 mg/dL in all animals.

The same dose of insulin induced a lower decrease in glycemia if we compare the results obtained from the first part of experiment, due to the increased basal glucose level.

Comparing the two glycemia profiles in the second part of the experiments, the one of ABA-treated mice was again significantly lower, with a significant reduction in the AUC of glycemia over the 4 hours monitoring period after insulin injection (Fig. 23).

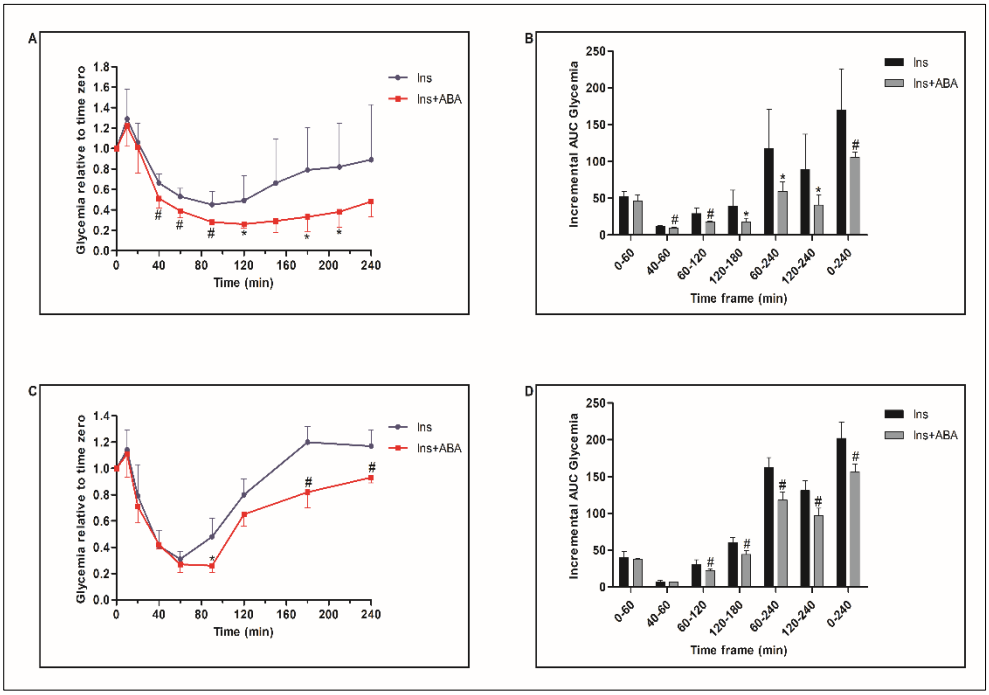

Figure 23. Glycemia profile after insulin administration to diabetic WT mice (and relative AUC).
LANCL1 WT mice divided into two groups (8 mice/group) were treated with a single high dose of STZ (200 mg/kg BW). When glycemia reached a value > 300 mg/dL, a first insulin test was performed with 0.1 U of insulin injected with or without ABA (5 µg/kg BW). Glycemia profile and AUC **(A - B upper panels)**. Similar insulin test with a glycemia > 500 mg/dL was performed. Glycemia profile and AUC **(C - D lower panels)**.
*p < 0.05 and #p < 0.02 relative to insulin.
P values are calculated by unpaired two-tailed t-test.

In agreement with data obtained before, the most marked glycemia profile reduction (in the ABA-treated animals) was observed in the timeframe 60–240 min.

Comparing the first and the second experiment, we observed higher percentages of reduction in the AUC in the ABA-treated vs. untreated mice; the percentage of AUC reduction observed in the timeframe 120–240 min, i.e., after the maximal effect of insulin was reached (between 60 and 90 min), was 50% in the first experiment and 25% in the second.

In both experiments, a significant reduction in the SD of the glycemia values relative to time zero was observed in the ABA-treated group, compared with controls, at all time-points starting from 60 min after insulin injection ($p = 0.004$ and $p = 0.02$ by paired t test, respectively)
These results indicate that a single oral dose of ABA, administered together with s.c. insulin, improves glycemic control by prolonging the reduction in glycemia after insulin administration; this effect occurs both under conditions of increased (300 mg/dL) and excess (>500 mg/dL) fasting glycemia, i.e., in the presence or absence, respectively, of residual endogenous insulin production after T1D induction. In addition, the reduced excursion of glycemia values among the ABA-treated mice, compared with controls, indicates a better glycemic control in the first group.

Chronic ABA Treatment Improves the Effect of Insulin in Hyperglycaemic T1D Mice

In order to test the effect of chronic ABA treatment on a condition of severe insulin deficient diabetes, mice were treated with a single high dose of STZ (200 mg/Kg BW, at time 0) and the oral ABA treatment (5 µg/Kg BW/day) was started at day 5, when glycemia values were ≥ 350 mg/dL.
Interestingly, ABA-treated mice showed a significant lowering in glycemia in the time frame from days 5 to 10; however, from the moment they reached a stable hyperglycaemia (500 mg/dL), we couldn't detect any significant difference between the two glycemia profiles (Fig. 24).
This observation suggests that in hyperglycaemia STZ-inducted, which mimics the absence of residual insulin secretion, ABA cannot substitute for the hormone; instead, when a small amount of residual insulin secretion is available, a synergism between the two hormones allows a reduction in glycemia, as already observed after the induction of diabetes with low-dose STZ (Fig. 24).

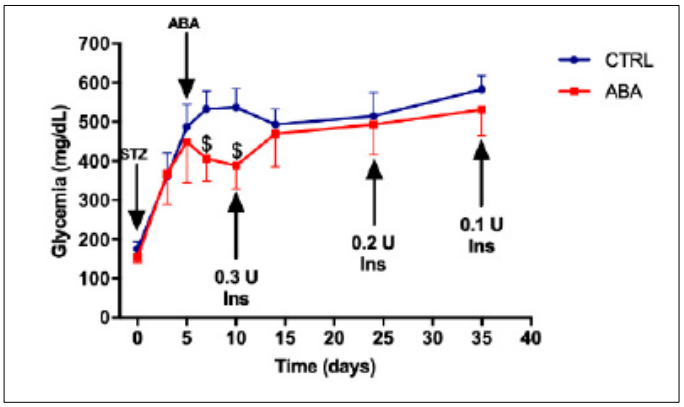

Figure 24. Glycemia profiles in WT diabetic mice.
LANCL2 WT mice were divided into two groups (10/group) and treated with a high-dose STZ (200 mg/kg BW) at time 0. After five days, the ABA treatment was started in one of the two groups. Three insulin tests (first, 0.3 U at day 10, 0.2 U at day 24, 0.1 U at day 35) were performed. Glycemia profile of the mice and timing of treatments with STZ, ABA and insulin.
$p < 0.005 relative to control.
P values are calculated by unpaired two-tailed t-test.

A first insulin test was performed at day 10, when ABA-treated mice showed a significantly lower glycemia as compared with controls (Fig. 25); two further insulin tests were performed when glycemia was ≥ 500 mg/dL in all animals.

In the three insulin tests, different insulin doses were used (Fig. 25), to test the effect on glycemia of the concomitant administration of a single oral dose of ABA.

In the first test, 0.3 U of insulin (12 mU/g BW) was injected s.c. in all animals; the ABA-treated group also received their daily dose of ABA (5 µg/Kg BW) orally, while the control group received an equal amount of water, and the glycemia profile was monitored until glycemia returned to pre-insulin levels in the control group.

In the second and third tests, the dose of insulin was reduced to 0.2 (8 mU/g BW) and 0.1 U (4 mU/g BW), respectively. With the highest dose of insulin (0.3 U), a significant difference between the glycemia profiles of the ABA-treated and control animals was observed between the time points 90 and 180 min (Fig. 25, upper left panel). The incremental AUC of glycemia was reduced in the ABA-treated animals compared with controls, particularly in the time frame 60–180 min after insulin injection (Fig. 25, upper right panel), and the total AUC over the time

span 0–240 min was approx. 30% lower in the ABA-treated mice, as compared with the control mice. When the dose of insulin administered was 0.2 U, the glycemia profile of the ABA-treated vs. ABA-untreated animals was again lower over the time frame 60–180 min (Fig. 25, central left panel), and the total AUC over the time span 0–180 min was reduced by approx. 20% in the ABA-treated mice, as compared with the control mice (Fig. 25, central right panel). Finally, when the dose of insulin was further reduced to 0.1 U, the glycemia profile of the ABA-treated mice was significantly lower than that of controls at each time point after 60 min from insulin administration (Fig. 25, lower left panel). The incremental AUC of glycemia was most significantly reduced in the time frame 60–180 min, and the total AUC over the time span 0–180 min was approx. 40% less than that of controls (Fig. 25, lower right panel). Collectively, these results indicate that treatment with ABA ameliorated the effect of exogenous insulin in a condition of complete endogenous insulin deficiency, prolonging the timeframe of reduced glycemia over the time span 60–180 min after insulin (and ABA) administration. The highest percentage of reduction in the glycemia AUC between 0 and 180 min (40%) in ABA-treated vs. control mice was observed with the lowest dose of insulin (0.1 U). In the first insulin test, basal glycemia was significantly different between ABA-treated and ABA-untreated mice, while in the second and third insulin tests basal glycemia was similar in the two groups of mice, indicating that, although treatment with ABA alone did not induce a reduction in glycemia, in combination with exogenous insulin, ABA increased the effect of the hormone.

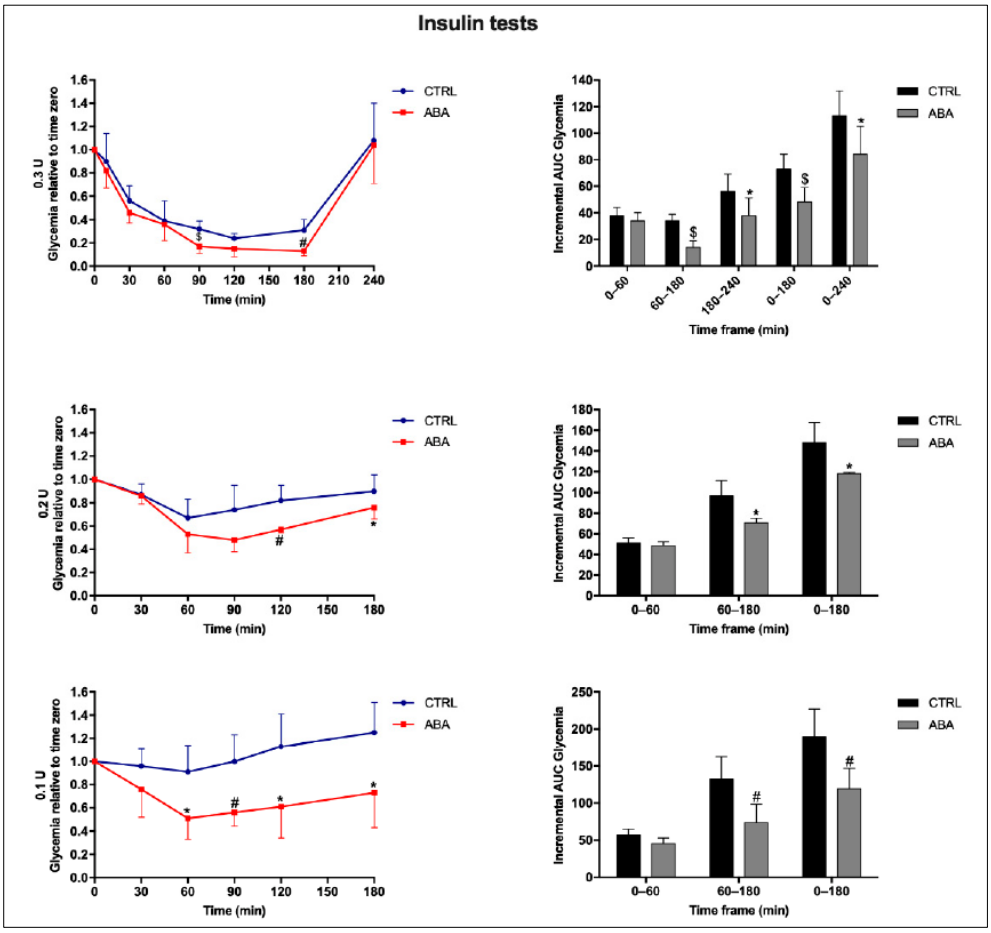

Figure 25. Insulin tests with different concentration of insulin in WT mice.
Glycemia profiles in CTRL and ABA-treated mice **(left panels)**. AUC of glycemia **(right panels)**.
*p < 0.05, #p < 0.05 and $p < 0.005 relative to control.
P values are calculated by unpaired two-tailed t-test.
For the endpoint of the glycemia profile the Mann-Whitney U test (one-tailed) was used, because the two data sets were not normally distributed.

Five days after the last insulin test, mice were sacrificed and basal insulinemia and pancreatic insulin mRNA were measured in all animals. Insulinemia values were not significantly different between ABA-treated and ABA-untreated mice, mean values were 0.22 ± 0.08 and 0.20 ± 0.09 µg/L, respectively, and were approx. 20 times lower than peak insulin levels in STZ-untreated WT mice undergoing a 1 g/Kg BW glucose load to induce transient hyperglycemia. Pancreatic insulin mRNA also was not significantly different between ABA-treated and ABA-untreated mice and was approx. 200 times lower than in STZ-untreated controls undergoing a 1 g/Kg BW glucose load (Fig. 26).

Although basal glycemia was not significantly different between ABA-treated and ABA-untreated mice at the end point of the experiment (Fig. 26), a statistically significant inverse correlation was observed between basal glycemia and plasma insulin in the ABA treated mice (Pearson R = −0.86, p = 0.001, n = 10), but not in the ABA-untreated mice (Pearson R = −0.62, p = 0.056, n = 10). Thus, apparently, on an individual basis, chronic treatment with ABA sensitized mice to the effect of residual endogenous insulin on basal glycemia, although the mean value of glycemia was not significantly different between the two groups of mice. Indeed, the insulin receptor mRNA was approx. 10 times more abundant in the skeletal muscle from ABA-treated mice as compared with control, ABA-untreated mice, and this occurred both in WT and in KO animals (Fig. 26). The increased expression of the insulin receptor in the SkM from ABA-treated mice likely also improved sensitivity to exogenous insulin, contributing to the reduction in glycemia in the ABA-treated mice during the insulin test.

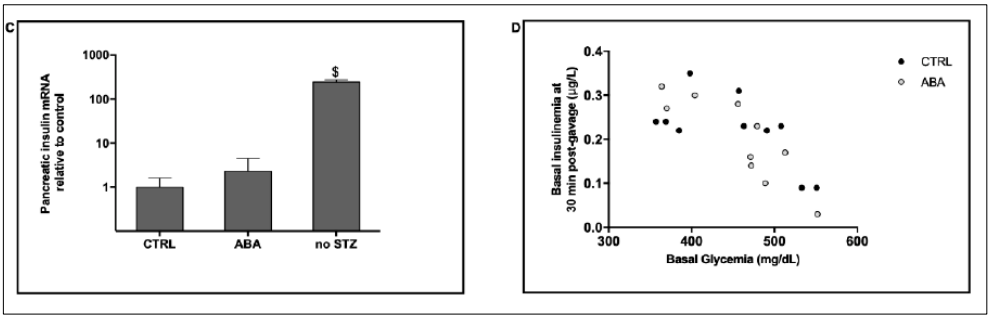

Figure 26. Pancreatic expression of insulin mRNA in WT mice.
Pancreatic insulin mRNA of STZ-treated and untreated animals (with or without ABA) **(C - left panel)**. Pearson correlation between basal glycemia and insulinemia in ABA-treated and untreated mice **(D - right panel)**.

LANCL2 KO Mice Respond to Chronic ABA with a Reduced Glycemia Profile

Even if LANCL1 has a lower affinity for ABA as compared with LANCL2, it also binds ABA and, similarly to LANCL2, it activates the AMPK/PGC-1a/Sirt1 signalling cascade in skeletal muscle, with a high expression of both GLUT1 and GLUT4 *(Spinelli S et al, 2021)*.

Interestingly, LANCL2 KO mice spontaneously overexpress LANCL1 in the SkM (approx. twice the amount of their WT siblings) *(Spinelli S. et al, 2021)*, allowing us to test whether LANCL1 could mediate the beneficial effect of chronic ABA treatment on hyperglycaemia induced by low-dose STZ.

LANCL2 KO mice underwent chronic treatment with oral ABA (5 µg/Kg BW/day), starting from day 0, and STZ administration started on day 5 for 5 consecutive days (20 mg/Kg BW/day). At the endpoint, on day 28, the mean glycemia of KO mice (294 ± 51 mg/dL) was significantly lower than that of the WT animals (395 ± 64 mg/dL, p = 0.029). Indeed, the glycemia profile of the ABA-treated KO animals was significantly reduced, as compared with that of untreated KO mice, starting from day 14 and until the end of the monitoring period (Fig. 27).

At day 28, we performed a final OGTT: ABA-treated KO mice showed a significantly reduced glycemic response with a smaller increase in glycemia after glucose load: consequently, we observed a decreased AUC of glycemia over the 90 min period of monitoring (Fig. 27).

Plasma insulin at 30 min post-gavage was not significantly different between ABA-treated and ABA-untreated LANCL2 KO mice (0.37 ± 0.12 vs. 0.40 ± 0.16 mg/L, respectively) and was similar to that measured in the LANCL2+/+ mice at the end of the similar experimental protocol (Fig. 27).

To complete the picture, we analysed expression levels of glycolytic enzymes in samples of quadriceps muscles from both WT and LANCL2 KO animals after mice sacrifice (2 days after OGTT, at the end of experiment).

Transcription of the glycolytic enzymes GaPDH and PFK1, and of the subunit 1 (E1) of the pyruvate dehydrogenase (PDH) complex, was significantly higher in the ABA-treated animals, as compared with the respective untreated controls, with no significant differences between WT and LANCL2 KO mice (Fig. 27), suggesting that ABA stimulates muscle glucose metabolism as well as glucose uptake.

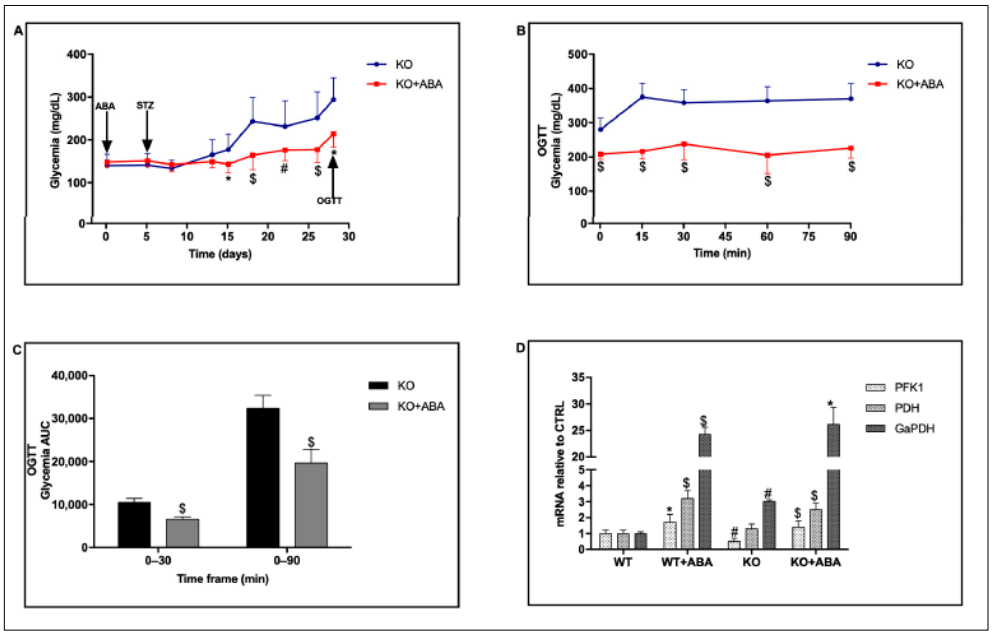

Figure 27. Glycemia profile before and after the OGTT (together with respective AUC), and mRNA expression levels of glycolytic enzymes in KO mice skeletal muscle.
Eight-week-old LANCL2 KO mice were divided into two groups (9/group) and then treated or not with ABA (5µg/kg BW/day) from day 0. After five days mice received, for 5 consecutive days, 20 mg/kg BW STZ. An OGTT was performed at day 28. Glycemia profile of KO mice treated or not with ABA and the timing of all the treatments **(A - upper left panel)**. Glycemia profile after OGTT **(B - upper right panel)**. AUC of glycemia in the indicated time frames after the OGTT **(C - lower left panel).** mRNA levels of glycolytic enzymes in the skeletal muscle of WT and KO mice after sacrifice (day 30) **(D - lower right panel)**.
*p < 0.05, #p < 0.02 $p < 0.005 relative to KO **(upper left panel)**.
$p < 0.005 relative to KO **(upper right panel)**.
$p < 0.005 relative to KO **(lower left panel)**.
GaPDH (#p < 0.02, $p < 0.005 relative to WT and *p < 0.05 relative to KO); PFK1 (*p < 0.05, #p < 0.02 relative to WT and $p < 0.005 relative to KO); PDH ($p < 0.005 relative to WT and KO) **(lower right panel)**.

mRNA levels of AMPK and PGC-1a were similar in KO (Fig. 28) and in WT mice, while GLUT4 transcription was approx. 2-fold higher in KO as compared with WT mice. Transcription of these genes was however significantly increased in KO mice treated with ABA (Fig. 28).

As detected by Western blot analysis, SkM from KO mice showed higher protein levels of PGC-1a and GLUT4 than WT controls, which did not further increase upon ABA treatment (excluding AMPK) and were similar to those of WT mice treated with ABA (Fig. 28). Finally, an approx. 10-fold stimulation by ABA of the transcription of the insulin receptor mRNA was also observed in LANCL2 KO mice treated with

ABA (Fig. 28). These results indicate that LANCL2 is dispensable for the beneficial effect of exogenous ABA on glycemia control in a diabetic condition induced by low-dose STZ; the effect of ABA in LANCL2 KO mice is likely mediated by (overexpressed) LANCL1, and the dose of exogenously administered ABA is sufficient to activate the signalling pathway downstream of LANCL1, confirming previous results *(Spinelli S. et al, 2021)*.

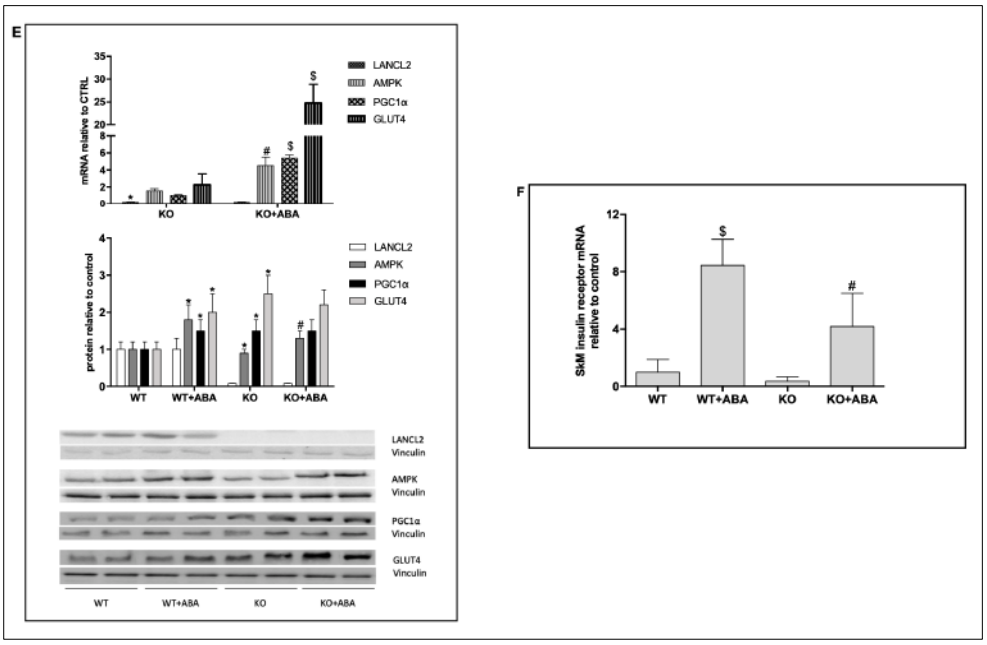

Figure 28. mRNA and protein expression of LANCL2, AMPK, PGC-1a, GLUT4 and insulin receptor in WT and KO mice.
mRNA levels of LANCL2, AMPK, PGC-1a, GLUT4 in the skeletal muscle of LANCL2 KO mice relative to untreated control mice **(E - upper left panel)**.
Protein expression, together with a representative Western Blot analysis, of LANCL2, AMPK, PGC-1a, GLUT4 relative to levels in untreated WT muscle **(E - lower left panel)**. Insulin receptor in skeletal muscle of LANCL2 WT and KO mice **(F - right panel)** p values are calculated by unpaired two-tailed t-test.
Values are the mean ± SD from 9 animals **(upper left panel)**.
Values are the mean ± SD from 5 animals; values were normalized on the housekeeping Vinculin (*$p < 0.05$ relative to WT, #$p < 0.02$ and \$$p < 0.005$ relative to KO) **(lower left panel)**.
\$$p < 0.005$ relative to WT, #$p < 0.02$ relative to KO) **(right panel)**.

These results indicate that in LANCL2 KO mice, a spontaneous overexpression of LANCL1 occurs in the skeletal muscle. Although LANCL2 KO mice show a reduced glucose tolerance as compared with WT mice, in line with the absence of one of the ABA

receptors, they respond to ABA treatment with a significant improvement of glucose tolerance.

This response can be attributed to the activation of the same AMPK/PGC1a-mediated signalling pathway also activated by LANCL2.

The ABA-LANCL1/2 system controls the mitochondrial proton gradient in H9c2 cardiomyocytes.

Cardiomyocytes are eminently aerobic cells, and their metabolism relies on glucose oxidation and oxygen consumption for energy production. The increased glucose uptake observed in ABA-treated, or in LANCL1/2-overexpressing L6 myoblasts described above, together with the increased mitochondrial respiration reported in ABA-treated adipocytes *(Sturla L. et al, 2017)* suggested to explore whether the ABA-LANCL1/2 system played a role in the mitochondrial function of cardiomyocytes.

The fluorescent dye JC-1 was used to explore the mitochondrial proton gradient (ΔΨ) in LANCL1/2-overexpressing vs. double silenced cells.

This fluorescent molecule accumulates within mitochondria and changes its emission from green to red as the ΔΨ increases *(Chen G. et al, 2018)*. As shown in Fig. 29, mitochondrial fluorescence was largely green, with just a trace of red, in LANCL1/2-silenced cells (row A). Conversely, mitochondrial fluorescence was predominantly red in the LANCL1/2-overexpressing cells. The calculated red/green ratio (Fig. 29) was almost 1 log higher in LANCL1/2 overexpressing vs. silenced cells. After incubation with ABA, the red fluorescence further increased in the overexpressing, but not in the silenced cells, indicating an increased ABA-sensitivity in the LANCL1/2 overexpressing vs. silenced cells. The red/green fluorescence ratio was approx. 1,2 and 2,8 in double silenced cells without or with ABA and approx. 10,2 and 15,3 in overexpressing cells, treated or not with ABA.

These results indicate that the LANCL1/2 level of expression positively affects mitochondrial respiration and consequently the mitochondrial proton gradient in cardiomyoblasts.

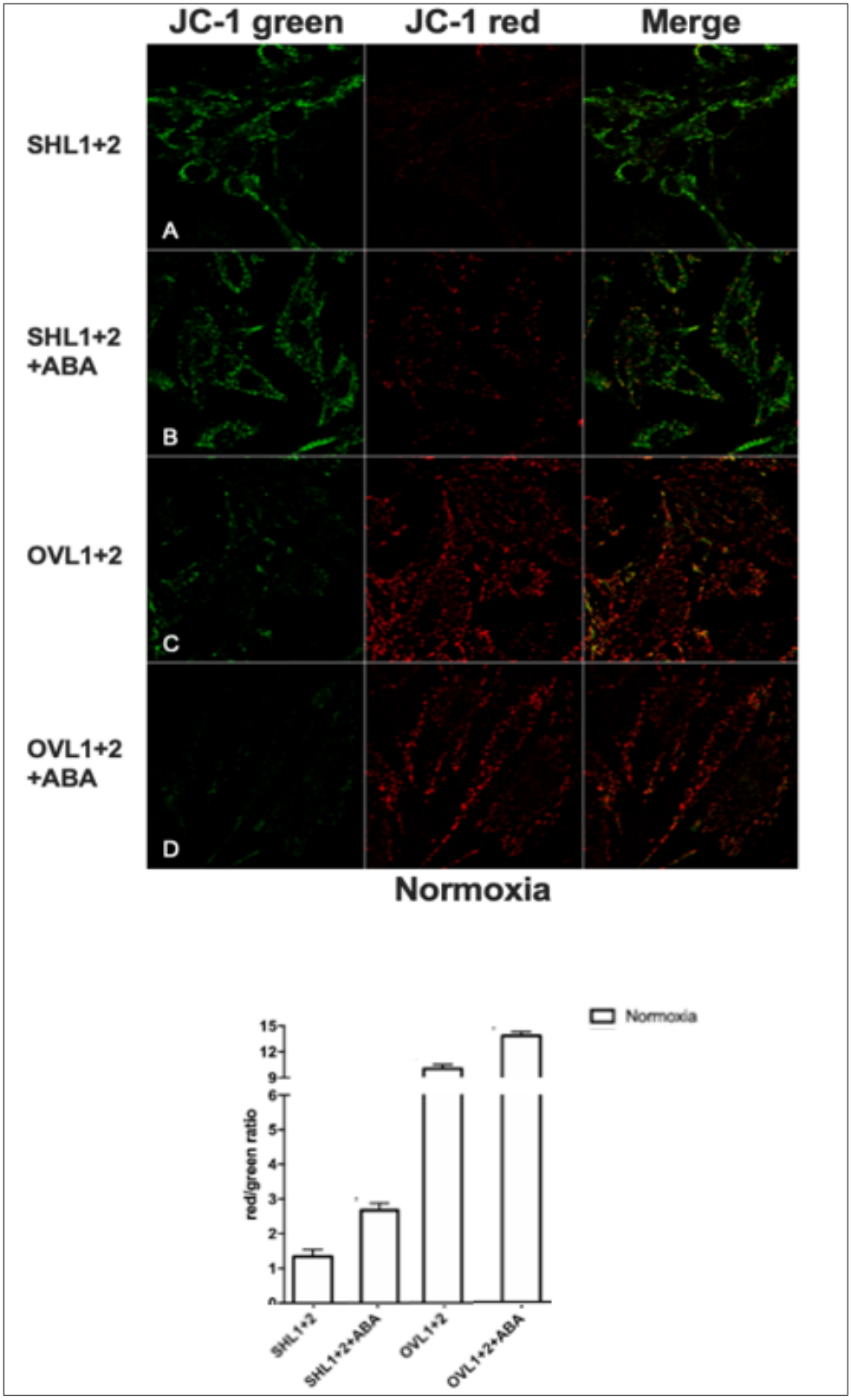

Figure 29. Functional mitochondria in normoxia in overexpressing and silenced cells.
Representative confocal microscopy images of H9c2 cells overexpressing LANCL1 and LANCL2 (OVL1+2), or double-silenced for both proteins (SHL1+2) in normoxia **(upper panel)**. Double-silenced cells, without or with ABA **(A – B upper panel)**; LANCL1/2-overexpressing cells without or with ABA **(C – D upper panel)**.
Red/green fluorescence ratio calculated for the experiments shown in the upper panel **(lower panel)**.
*p < 0.01 relative to untreated control cells and $p < 0.05 relative to ABA-treated control cells by unpaired t test.
The mean ± SD of the red/green fluorescence ratio was always calculated at least 3 microscopic fields.

DISCUSSION

Diabetes

Overview

Diabetes is now considered a pathology with epidemic proportions: according to the statistics represented in Fig. 10 and dating back to the 2016 by WHO *(https://www.aogoi.it/notiziario/archivio-news/oms-cause-morte/)*, diabetes is the seventh leading cause of death worldwide. In 2022, approximately 537 million adults are living with diabetes and the number is expected to rise over the years *(International Diabetes Federation)*.

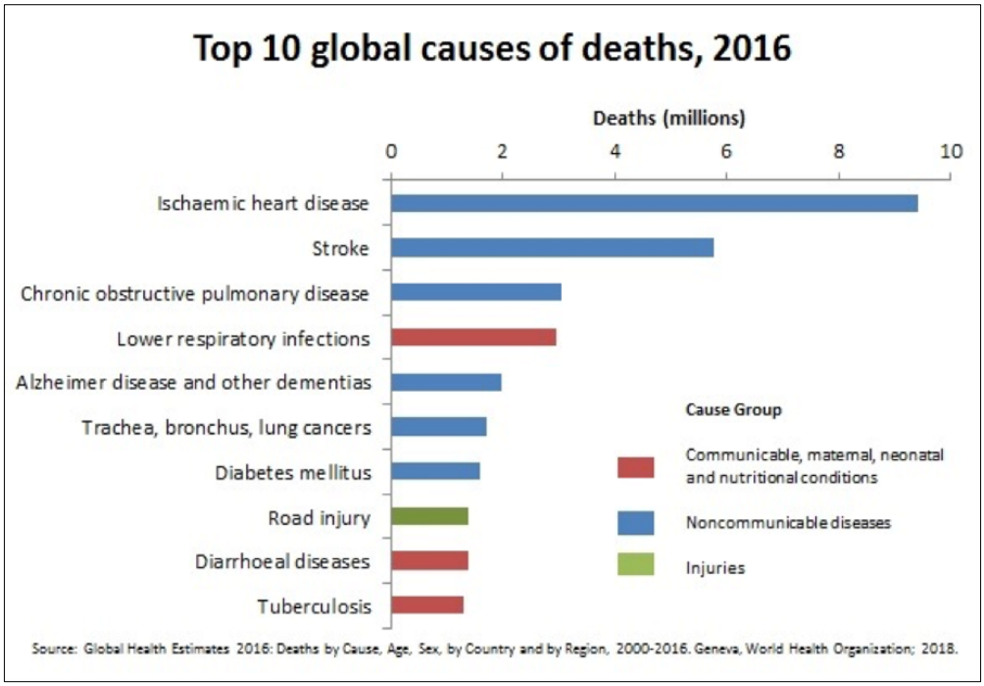

Figure 30. Top ten global causes of death divided in 3 groups, 2016.
Graphic that represents the proportions of deaths (millions) in 2016.

Type 1 Diabetes (T1D)

T1D is an autoimmune disease that destroys pancreatic β-cells (the mechanism is explained in Fig. 31) leading to endogenous insulin deficiency and consequently to hyperglycaemia *(WHO) (DiMeglio L.A. et al, 2018)*. The body transforms dietary carbohydrates in blood glucose; given that there is not enough insulin, glucose is not taken up by cells and its blood level remains high. Living an active lifestyle with a healthy diet and physical activity, together with insulin therapy, patients can live a normal life *(International Diabetes Federation)*.

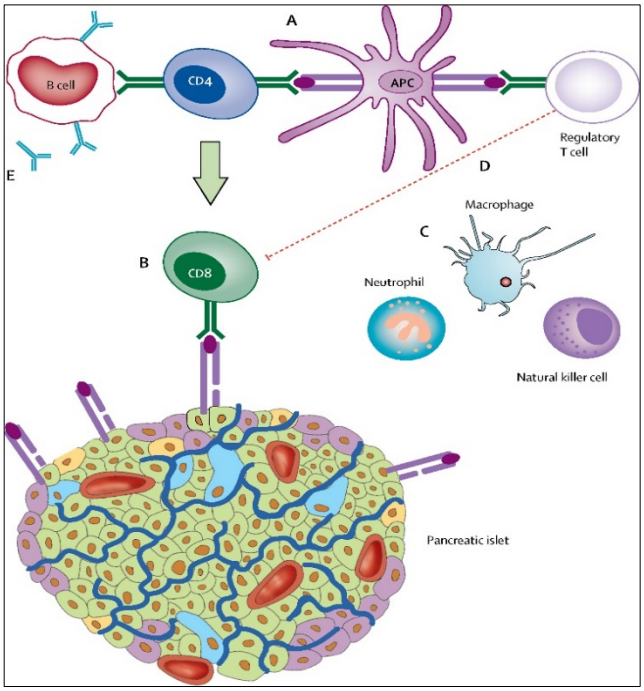

Figure 31. Type 1 diabetes.
Mechanism of T1D as an autoimmune disease. *(DiMeglio L. A. et al, 2018)*

Type 2 Diabetes (T2D)

This is the most common type of diabetes (around 90% of the cases) *(International Diabetes Federation)* and it is characterized by insulin-resistance rather than insulin deficiency, at least for several decades during which pancreatic β-cell activity is excessively stimulated by basal hyperglycemia *(Wu Y. et al, 2014)*: insulin is not able to reduce the blood glucose level until the pancreas is totally exhausted and doesn't produce insulin anymore (as represented in Fig. 32). The most

common risk factors for developing T2D are the following *(International Diabetes Federation)*:

- Family history of T2D
- Overweight
- Unhealthy diet
- Sedentary lifestyle
- High Blood pressure
- Impaired glucose tolerance.

It is evident that diabetes is closely related to cardiovascular diseases, that is among the sequelae of this disease.

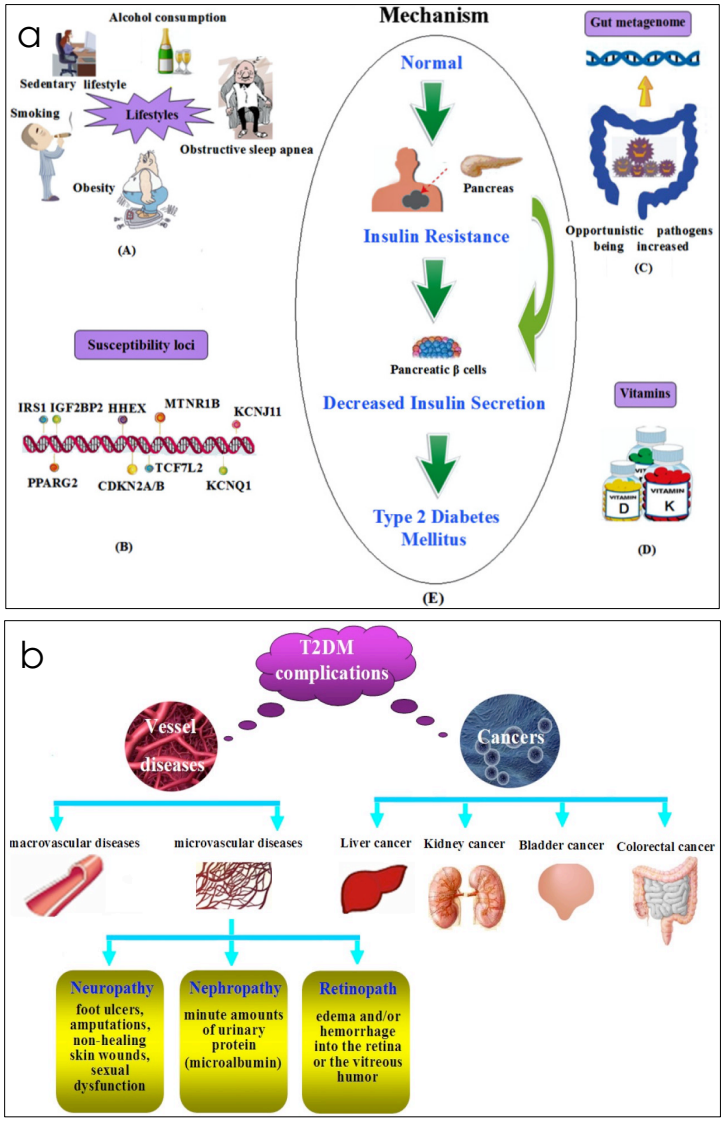

Figure 32. Type 2 Diabetes.
The pathogenesis of T2D with the risk factors **(a)** and Diabetes complications **(b)** *(Wu Y et al. 2014)*

Gestational Diabetes (GDM)

GDM is the second most frequent complication of gestation, after hypertension. GDM occurs in 2-10% of pregnant women without a history of diabetes. After childbirth, the majority of women with GDM returns to normal blood glucose levels but 5-10% of women with GDM maintain high blood glucose levels developing T2D. A history of GDM is among the risk factors for developing T2D in later years.

Prediabetes

Overview

The ADA lay definition of prediabetes is "a condition where blood sugar levels are higher than normal, but not yet high enough to be diagnosed as diabetes" *(American Diabetes Association)*. This condition is a sort of intermediate state of hyperglycaemia *(Bansal N., 2015)* and exposes affected subjects to a higher risk of developing diabetes. However, this condition is reversible *(American Diabetes Association)*: in fact, having prediabetes does not necessarily imply that you will develop overt T2D in the future, if you make a significant lifestyle change in terms of diet and physical activity (unfortunately these recommendations have a low compliance because patients do not perceive a real danger to their health when they are in the prediabetic stage).
Even if the cornerstone to delay or prevent onset of T2D are lifestyle interventions, a pharmacological treatment can be used to prevent the conversion of prediabetes to diabetes *(Hostalek U. et al, 2015)*.

Current pharmacological therapy for prediabetes

The current most widely employed drug is metformin, which is also an antidiabetic treatment *(Hostalek U. et al, 2015)*. Metformin seems to prevent the development of diabetes in 45% of the cases *(Lily M. et al, 2009) (Sanchez-Randel E. et al, 2017)* and also improves the cholesterol profile and the BMI, at least in the short term, i.e. within the first 6 months of treatment. Unfortunately, at 12 months there's no

difference between treated and untreated cases. Besides metformin, there are also glitazones, which decrease the risk of diabetes by 60% over 3 years *(Dagenais G.R. et al, 2008) (Gerstein H.C. et al, 2006)*. Other alternatives are: a-glucosidase inhibitors, GLP-1 analogues, and inhibitors of renal tubular glucose reabsorption.

Unfortunately, all these drugs have multiple side effects, including an increase in body weight. For this reason, pharmacologic therapy in prediabetes is recommended only for high-risk patients (or patients who have no improvements after lifestyle changes).

Nutraceuticals in prediabetes

There are around 450 medicinal plants that have antidiabetic effect, but the mechanism of action is understood for only a few of them *(Prabhakar P.K. et al, 2008)*.

The interest in this type of therapy comes from the efficacy of some of these products, with the added value of absence of side effects and low cost *(Prabhakar P.K. et al, 2011)*. In Fig. 33, some plants with antidiabetic effect are listed: they contribute to the hypoglycaemic activity stimulating insulin production and reducing the intestinal glucose uptake *(Prabhakar P.K. et al, 2011)*.

Category	Target tissue and mode of action	Conventional drug	Natural medicine
Hypoglycemic agents	Pancreas (Increase insulin secretion)	Sulphonylurea, miglitinides	Banaba (*Lagerstroemia speciosa*) Bitter melon (*Momordica charantia*) Fenugreek (*Trigonella foenum-graecum*) Gymnema (*Gymnema sylvestre*)
Insulin sensitizers	Liver (Decrease glucose production); Adipose tissue and skeletal muscles (Increase peripheral glucose uptake)	Metformin, thiazolidinedione	Agaricus mushroom (*Agaricus blazei*) American ginseng (*Panax quinquefolius*) Banaba (*Lagerstroemia speciosa*) Cassia cinnamon (*Cinnamomum aromaticum*) *Panax ginseng* Prickly pear cactus (*Opuntia ficus-indica*) Soy (*Glycine max*) Vanadium
Carbohydrate absorption inhibitors	Intestine (Decrease glucose absorption)	α -glucosidase inhibitor	Bean pod (*Phaseolus vulgaris*) Blond psyllium (*Plantago ovata*) Fenugreek (*Trigonella foenum-graecum*) Glucomannan (*Amorphophallus konjac*) Guar gum (*Cyamopsis tetragonoloba*) Oat bran (*Avena sativa*) Prickly pear cactus (*Opuntia ficus-indica*) Soy (*Glycine max*) White mulberry (*Morus alba*)
Miscellaneous		Exenatide (Byetta), Pramlintide (Symlin), Saxagliptin (Onglyza), Sitagliptin (Januvia)	Alpha-lipoic acid Chia (*Salvia hispanica*) Coenzyme Q10 Selenium Stevia (*Stevia rebaudiana*)

Figure 33. Natural medicine plants.
Most common medicinal plants used against glucose intolerance and their mechanism of action. *(Prabhakar P.K. et al, 2011)*

ABA as a nutraceutical supplement for glycemia control

Data presented in this thesis, along with previously published studies, allow to conclude that the ABA/LANCL1-2 hormone/receptors system plays an important in glycemia control and glucose tolerance in mammals.

Murine studies on ABA-treated mice and clinical studies on prediabetic and on borderline subjects demonstrate that chronic ABA treatment improves basal glycemia, reduces peak glycemia after glucose load and improves glucose tolerance, lipidaemia and body weight *(Magnone M. et al, 2018) (Derosa G. et al, 2020)*.

Interestingly, the action of ABA is independent from insulin: ABA activates a different signalling pathway, and its effect can synergize with that of residual endogenous, as well as exogenously administered insulin *(Magnone M. et al, 2022)*.

In vivo, the dietary ABA intake reduces glycemia levels after the OGTT in both humans and rodents *(Magnone M. et al, 2015)* and, interestingly plasma insulin levels are reduced, suggesting that ABA treatment reduces the necessity for endogenous insulin release.

The signalling pathway activated by the ABA/LANCL1-2 hormone/receptors system in skeletal muscle and in adipocytes involves the AMPK/PGC1a/Sirt1 axis (Fig. 34), which in turn controls GLUT4 and GLUT1 expression and membrane translocation, glucose oxidation, NAD+ synthesis, mitochondrial biogenesis, respiration, and proton gradient, ultimately leading to an increased energy metabolism in skeletal muscle and in adipose tissue. In adipocytes, the ABA/LANCL system stimulates browning of white adipocytes and mitochondrial uncoupling in brown adipocytes *(Sturla L. et al, 2017)*.

The increase in energy metabolism in skeletal muscle and in adipose tissue, which account for the largest combined whole-body energy expenditure, is likely responsible for the observed beneficial effect of exogenous ABA in borderline and in prediabetic subjects *(Magnone M. et al, 2018) (Derosa G. et al, 2020)*.

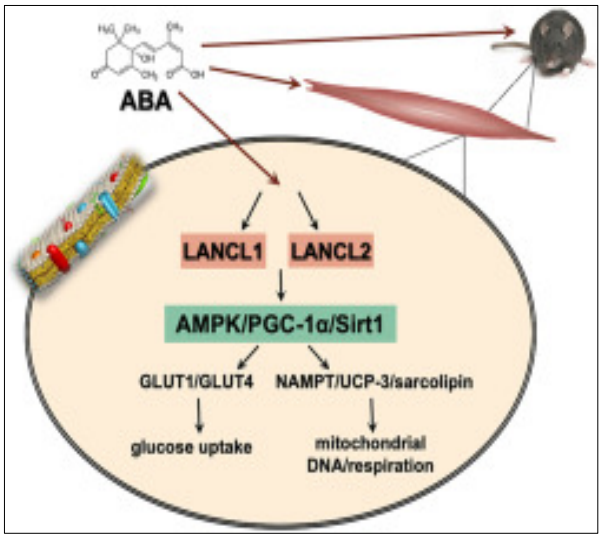

Figure 34. ABA signalling pathway through LANCL1/LANCL2 in skeletal muscle. The signalling pathway through ABA receptors activates the AMPK/PGC-1α/SIRT1 axis that respectively leads to glucose uptake (through GLUT1/4) and mitochondrial respiration (through NAMPT/UCP3/sarcolipin) *(Spinelli S. et al, 2021)*.

Both LANCL 1 and LANCL2 exert a transcriptional control on AMPK, PGC-1a, and Sirt1: this axis is important for several functions like mitochondrial biogenesis and fusion, muscle contractility and recovery of muscle function caused by disuse or ageing *(Zeng M. et al, 2014)* and protection of muscle cells against nutrient deprivation or ischemia-reperfusion injury *(Ma L. et al, 2020) (Tang J. et al, 2019)*.

The ABA/LANCL1-2 system controls energy expenditure

The first evidence that the ABA/LANCL system could influence the mitochondrial respiration was obtained in adipocytes *(Sturla L. et al, 2017)*. Then, other evidence was obtained both in skeletal muscle and cardiac muscle.

- Adipose Tissue: ABA treatment has some important outputs in 3T3 cells-derived adipocytes, like increase of O_2 consumption, transcription of "browning genes" (like UCP-1); besides, chronic ABA treatment is linked to the increase of mitochondrial DNA content in white adipocytes and UCP-1 expression in brown adipocytes in mice *(Sturla L. et al, 2017)*.

- Skeletal muscle: in murine L6 myoblasts, the consequences of the ABA receptor overexpression are the stimulation of mitochondrial respiration and the expression of skeletal muscle uncoupling proteins (like sarcolipin and UCP3) *(Spinelli S. et al, 2021)*.
- Cardiac muscle cells: overexpression of ABA receptors leads to an increase of O_2 consumption, as compared with silenced cells (Figure 29).

These tissues plus the brain are the perfect examples of metabolic oxidative capacity.

The key regulator of these metabolic reactions is PGC-1a: this protein has been identified as a "mediator of the transcriptional outputs triggered by metabolic sensors" *(Cantò C. et al, 2009)*. PGC-1a is induced under conditions that require increased energy production, such as cold, fasting and exercise.

The effect downstream of activated PGC-1a are:

- mitochondrial biogenesis
- respiration rate
- energy expenditure
- co-activator of some important transcription factors like nuclear receptors for several hormones (the thyroid hormone receptor TR, glucocorticoid receptors GRs, estrogen receptors ERs and estrogen-related receptors ERRs).

The signals from AMPK and Sirt1 are immediately modified at transcriptional level via phosphorylation and deacetylation, respectively.

It is not surprising that a dysfunctional AMPK/PGC-1a/Sirt1 signaling axis should be responsible for reduced muscle energy expenditure, as occurs in aging and in metabolic disorders, such as T2D *(Zhang J. et al, 2021)*. Consequently, pharmacological activation of this pathway holds promise as a new strategy to protect muscle and heart function under conditions that reduce myocyte vitality (aging, hypoxia,

diabetes) *(Gan L. et al, 2020) (Luo G. et al, 2019) (Tian L. et al, 2019) Fang Y. et al, 2021) (Hu L. et al, 2014)*.

The results described here could have clinical implications in diabetic cardiomyopathy, a heart condition associated with both T1D and T2D. The metabolic hallmarks of the diabetic heart are reduced insulin-mediated mitochondrial glucose oxidation and increased free fatty acid uptake, which impairs mitochondrial fatty acid oxidation, resulting in mitochondrial dysfunction, energy depletion and accumulation of toxic lipid metabolites *(Tan Y. et al, 2020)*. Defective endogenous ABA has been observed in both T1D and T2D *(Bruzzone S. et al, 2012) (Ameri P. et al, 2015)*, suggesting that endogenous ABA deficiency may play a role in the pathogenesis of glucose intolerance due to insulin deficiency or resistance.

Indeed, oral ABA has been shown to improve glucose tolerance in borderline and in prediabetic subjects *(Magnone M. et al, 2018) (Derosa G. et al, 2020)* and to improve insulin sensitivity in murine models of T1D *(Magnone M. et al, 2022)*. From the data presented here, we could hypothesize that the impaired endogenous ABA function occurring in diabetes could contribute to a reduced function of cardiomyocyte mitochondria, arguably the most important organelle for cell energy production.

These results warrant further studies aimed at exploring a cardioprotective effect of oral ABA, particularly in the diabetic condition. In fact, current strategies to reduce acute ischemia/reperfusion injury advocate the stimulation of glycolysis via AMPK activation, of mitochondrial glucose oxidation, of NAMPT activity, and the elevation of the levels of Sirt1/Sirt3 *(Eid R.A. et al, 2020) (Hsu C.P. et al, 2009)*, all effects observed downstream of the ABA/LANCL signaling pathway on muscle cells. In addition, ABA stimulates release of ATP from human erythrocytes *(Vigliarolo T. et al, 2015)*, which in turn exerts vasodilating effects, which should further improve the recovery of mitochondrial respiration after ischemia.

CONCLUSIONS

Does exogenous ABA reduce hyperglycemia in multiple low-dose streptozotocin STZ-treated mice? The answer is yes it does, which means that in the presence of a markedly reduced endogenous insulin production ABA supplementation could improve the function of, and sensitivity to, residual insulin.

Does ABA improve the effect of suboptimal doses of insulin in single high-dose STZ-treated mice? Again, the answer is yes it does. In the absence of endogenous insulin, ABA alone does not control glycemia; however, in addition to insulin, ABA supplementation allows to reduce the dose of insulin required for glycemia control.

Can LANCL1 substitute for LANCL2 in mediating the effect of ABA on the skeletal muscle in diabetic mice? The answer is yes, indicating a redundancy of ABA receptors, which may find its explanation in the pivotal role played by the ABA/LANCL1-2 system in controlling energy metabolism in muscle, adipose and heart cells.

Finally, which effect does overexpression or silencing of LANCL1 and LANCL2 have on the mitochondrial proton gradient of the murine cardiomyoblast cell line H9c2? Both LANCL proteins indeed control mitochondrial function, as their combined silencing drastically reduces and their overexpression instead significantly increases the mitochondrial proton gradient, which is the result of the metabolic and respiratory activity of cardiomyocytes.

Collectively, these results warrant clinical studies aimed at verifying whether oral ABA supplementation could improve glucose tolerance in diabetic patients, at the same time increasing cardiomyocyte resilience to diabetes-induced loss of function.

BIBLIOGRAPHY/SITOGRAPHY

A

Alessi D.R., James S.R., Downes C.P., Holmes A.B., Gaffney P.R., Reese C.B., Cohen P. (1997) Characterization of a 3-phosphoinositide-dependent protein kinase which phosphorylates and activates protein kinase Balpha. Curr Biol. 1;7(4):261-9

Ameri P., Bruzzone S., Mannino E., Sociali G., Andraghetti G., Salis A., Ponta M.L., Briatore L., Adami G.F., Ferraiolo A., Venturini P.L., Maggi D., Cordera R., Murialdo G., Zocchi E. Impaired increase of plasma abscisic acid in response to oral glucose load in type 2 diabetes and in gestational diabetes. (2015). PLoS One 27;10(2):e0115992,

B

Bansal N. (2015). Prediabetes diagnosis and treatment: A review. World J Diabetes. 15;6(2):296-303

Bauer H., Mayer H., Marchler-Bauer A., Salzer U., Prohaska R. (2000). Characterization of p40/GPR69A as a peripheral membrane protein related to the lantibiotic synthetase component C. Biochem Biophys Res Commun. 18;275(1):69-74

Bodrato N., Franco L., Fresia C., Guida L., Usai C., Salis A., Moreschi I, Ferraris C., Verderio C., Basile G., Bruzzone S., Scarfì S., De Flora A., Zocchi E. (2009). Abscisic acid activates the murine microglial cell line N9 through the second messenger cyclic ADP-ribose. J. Biol Chem. 284(22):14777-87

Bruzzone S., Moreschi I., Usai C., Guida L., Damonte G., Salis A., Scarfì S., Millo E., De Flora A., Zocchi E. (2007). Abscisic acid is an endogenous

cytokine in human granulocytes with cyclic ADP-ribose as second messenger. PNAS; 3;104(14):5759-64

Bruzzone S., Bodrato N., Usai C., Guida L., Moreschi I., Nano R., Antonioli B., Fruscione F., Magnone M., Scarfì S., De Flora A., Zocchi E. (2008) Abscisic acid is an endogenous stimulator of insulin release from human pancreatic islets with cyclic ADP ribose as second messenger. J Biol Chem. 21;283(47):32188-97

Bruzzone S., Ameri P., Briatore L., Mannino E., Basile G., Andraghetti G., Grozio A., Magnone M., Guida L., Scarfì S., Salis A., Damonte G., Sturla L., Nencioni A., Fenoglio D., Fiory F., Miele C., Beguinot F., Ruvolo V., Bormioli M., Colombo G., Maggi D., Murialdo G., Cordera R., De Flora A., Zocchi E. (2012). The plant hormone abscisic acid increases in human plasma after hyperglycemia and stimulates glucose consumption by adipocytes and myoblasts. FASEB J. 26(3):1251-60

C

Cannon B., Nedergaard J. (2004). Brown adipose tissue: function and physiological significance. Physiol Rev. 84(1):277-359

Cantò C., Auwerx J. (2009). PGC-1alpha, SIRT1 and AMPK, an energy sensing network that controls energy expenditure. Curr Opin Lipidol. 20(2):98-105.

Cea M., Cagnetta A., Adamia S., Acharya C., Tai Y.T., Fulciniti M., Ohguchi H., Munshi A., Acharya P., Bhasin M.K., Zhong L., Carrasco R., Monacelli F., Ballestrero A., Richardson P., Gobbi M., Lemoli R.M., Munshi N., Hideshima T., Nencioni A., Chauhan D., Anderson K.C. (2016). Evidence for a role of the histone deacetylase SIRT6 in DNA damage response of multiple myeloma cells. Blood. 3;127(9):1138-50

Chen G., Yang Y., Xu C., Gao S. (2018). A flow cytometry-based assay for measuring mitochondrial membrane potential in cardiac myocytes after hypoxia/reoxygenation. J. Vis Exp (137):57725

Cichero E., Fresia C., Guida L., Booz V., Millo E., Scotti C., Iamele L., de Jonge H., Galante D., De Flora A., Sturla L., Vigliarolo T., Zocchi E., Fossa P. (2018). Identification of a high affinity binding site for abscisic acid on human lanthionine synthetase component C-like protein 2. Int J Biochem Cell Biol. 97:52-61

Cinti S. (2002). Adipocyte differentiation and transdifferentiation: plasticity of the adipose organ. J Endocrinol Investig. 25(10):823-35

Costford S.R., Brouwers B., Hopf M.E., Sparks L.M., Dispagna M., Gomes A.P., Cornnell H.H., Petucci C., Phelan P., Xie H., Yi F., Walter G.A., Osborne T.F., Sinclair D.A., Mynatt R.L., Ayala J.E., Gardell S.J., Smith S.R. (2018). Skeletal muscle overexpression of nicotinamide phosphoribosyl transferase in mice coupled with voluntary exercise augments exercise endurance. Mol. Metab. 7:1-11

D

Derosa G., Maffioli P., D'Angelo A., Preti P., Tenore G., Novellino E. (2020). Abscisic Acid Treatment in Patients with Prediabetes. Nutrients. 24;12(10):2931.

Dimeglio A.L., Evans-Molina C., Oram R.A. (2018). Type 1 diabetes. Lancet. 16;391(10138):2449-2462

DREAM (Diabetes REduction Assessment with ramipril and rosiglitazone Medication) Trial Investigations, Dagenais G.R., Gerstein H.C., Holman R., Budaj A., Escalante A., Hedner T., Keltai M., Lonn E., McFarlane S., McQueen M., Teo K., Sheridan P., Bosch J., Pogue J., Yusuf S. (2008). Effects of ramipril and rosiglitazone on

cardiovascular and renal outcomes in people with impaired glucose tolerance or impaired fasting glucose: results of the Diabetes REduction Assessment with ramipril and rosiglitazone Medication (DREAM) trial. Diabetes Care. 31(5):1007-14

DREAM (Diabetes REduction Assessment with ramipril and rosiglitazone Medication) Trial Investigators; Gerstein H.C., Yusuf S., Bosch J., Pogue J., Sheridan P., Dinccag N., Hanefeld M, Hoogwerf B., Laakso M., Mohan V., Shaw J., Zinman B., Holman R. R. (2006). Effect of rosiglitazone on the frequency of diabetes in patients with impaired glucose tolerance or impaired fasting glucose: a randomised controlled trial. Lancet. 23;368(9541):1096-105

Dutta D., Lai K.Y., Ordoñez A.R., Chen J., van der Donk W.A. (2018). Lanthionine synthetase C-like protein 2 (LanCL2) is important for adipogenic differentiation. J Lipid Res. 59(8):1433-1445

E

Eid R.A., Bin-Meferij M.M., El-Kott A.F., Eleawa S.M., Zaki M.S.A., Al-Shraim M., El-Sayed F., Eldeen M.A., Alkhateeb M.A., Alharbi S.A., Aldera H., Khalil MA. (2020). Exendin-4 protects against myocardial ischemia-reperfusion injury by upregulation of SIRT1 and SIRT3 and activation of AMPK. J Cardiovasc Trans Res. 14(4):619-635.

F

Fang Y., Wang X., Yang D., Lu Y., Wei G., Yu W., Liu X., Zheng Q., Ying J., Hua F. (2021). Relieving Cellular Energy Stress in Aging, Neurodegenerative, and Metabolic Diseases, SIRT1 as a Therapeutic and Promising Node. Front Aging Neurosci. 20;13:738686.

Fresia C., Vigliarolo T., Guida L., Booz V., Bruzzone S., Sturla L., Di Bona M., Pesce M., Usai C., De Flora A., Zocchi E. (2016). G-protein coupling

and nuclear translocation of the human abscisic acid receptor LANCL2. Sci. Rep. 25;6:26658

G

Gan L., Xie D., Liu J., Bond Lau W., Christopher T.A., Lopez B., Zhang L., Gao E., Koch W., Ma X.L., Wang Y. Small Extracellular Microvesicles Mediated Pathological Communications Between Dysfunctional Adipocytes and Cardiomyocytes as a Novel Mechanism Exacerbating Ischemia/Reperfusion Injury in Diabetic Mice. Circulation (2020). 24;141(12):968-983

Gomez-Cadenas A., Vives V., Zandalinas S.I., Manzi M., Sanchez-Perez A.M., Perez-Clemente R.M., Arbona V. (2015). Abscisic acid: a versatile phytohormone in plant signalling and beyond. Curr. Protein Pep. 16(5):413-34

Guri A.J., Hontecillas R., Si H., Liu D., Bassaganya-Riera J. (2007). Dietary abscisic acid ameliorates glucose tolerance and obesity-related inflammation in db/db mice fed high-fat diets. Clin Nutr. 26(1):107-16

Guri A.J., Hontecillas R., Ferrer G., Casagran O., Wankhade U., Noble A.M., D.L. Eizirik, Ortis F., Cnop M., Liu D., Si H., Bassaganya-Riera J. (2008) Loss of PPAR gamma in immune cells impairs the ability of abscisic acid to improve insulin sensitivity by suppressing monocyte chemoattractant protein-1 expression and macrophage infiltration into white adipose tissue. J. Nutr Biochem. 19(4):216-28

Guri A.J., Misyak S.A., Hontecillas R., Hasty A., Liu D., Si H., Bassaganya-Riera J. (2010). Abscisic acid ameliorates atherosclerosis by suppressing macrophage and CD4+ T cell recruitment into the aortic wall. J Nutr Biochem. 21(12):1178-85

H

He C., Zeng M., Dutta D., Koh T.H., Chen J., van der Donk W.A. (2017). LanCL proteins are not Involved in Lanthionine Synthesis in Mammals. Sci Rep. 20;7:40980

Hey S.J., Byrne E., Halford N.G. (2010). The interface between metabolic and stress signalling. Ann. Bot. 105(2):197-203

Hostalek, U., Gwilt M., Hildemann S. (2015). Therapeutic use of Metformin in Prediabetes and Diabetes prevention. Drugs. 75(10):1071-94

Hsu C.P., Oka S., Shao D., Hariharan N., Sadoshima J. Nicotinamide phosphoribosyl transferase regulates cell survival through NAD^+ synthesis in cardiac myocytes. (2009). Circ Res. 28;105(5):481-91.

Hu L., Zhou L., Wu X., Liu C., Fan Y., Li Q. (2014). Hypoxic preconditioning protects cardiomyocytes against hypoxia/reoxygenation injury through AMPK/eNOS/PGC-1a signaling pathway. Int J Clin Exp Pathol. 15;7(11):7378-88.

K

Katoh M., Katoh M. (2003). Identification and characterization of human ZPBP-like gene in silico. Int J Mol Med. 12(3):399-404

King A.J.F., Daniels Gatward L.F., Kennard M.R. (2020). Practical considerations when using mouse models of diabetes. Methods Mol Biol. 2128:1-10

L

Landlinger C., Salzer U., Prohaska R. (2006). Myristoylation of human LanC-like protein 2 (LANCL2) is essential for the interaction with the

plasma membrane and the increase in cellular sensitivity to Adriamycin. Biochim Biophys Acta. 1758(11):1759-67

Le Page-Degivry M.T., Bidard J.N., Rouvier E., Bulard C., Lazdunski M. (1986) Presence of abscisic acid, a phytohormone, in the mammalian brain. PNAS; 83(4):1155-8

Lee H.C., Walseth T.F., Bratt G.T., Hayes R.N., Clapper D.L. (1989). Structural determination of a cyclic metabolite of NAD+ with intracellular Ca2+-mobilizing activity. J Biol Chem. 25;264(3):1608-15

Lee J.O., Lee S.K., Jung J.H., Kim J.H., You G.Y., Kim S.J., Park S.H., Uhm K.O., Kim H.S. (2011). Metformin induces Rab4 through AMPK and modulates GLUT4 translocation in skeletal muscle cells. J Cell Physiol. 226(4):974-81

Lily M., Godwin M. (2009). Treating prediabetes with metformin: systematic review and meta-analysis. Can Fam Physician. 55(4):363-9

Lin B.L., Wang H.J., Wang J.S., Zaharia L.I., Abrams S.R. (2005). Abscisic acid regulation of heterophylly in Marsilea quadrifolia L.: effects of R - (-) and S - (+) isomers. J.Exp. Bot.; 56(421):2935-48

Liu X., Yue Y., Li B., Nie Y., Li W., Wu W.H., Ma L. (2007). A G-protein coupled receptor is a plasma membrane receptor for the plant hormone abscisic acid. Science. 315(5819):1712-6

Livak K.J., Schmittgen T.D. (2001). Analysis of relative gene expression data using real time quantitative PCR and the 2ΔΔC(t) Method. Methods. 25(4):402-8

Luo G., Jian Z., Zhu Y., Zhu Y., Chen B., Ma R., Tang F., Xiao Y. Sirt1 promotes autophagy and inhibits apoptosis to protect

cardiomyocytes from hypoxic stress. (2019) Int J Mol Med. 43(5):2033-2043.

M

Ma L., Wang R., Wang H., Zhang Y., Zhao Z. (2020). Long-term caloric restriction activates the myocardial SIRT1/AMPK/PGC-1a pathway in C57BL/6J male mice. Food & Nutrition Research 29:64

Magnone M., Bruzzone S., Guida L., Damonte G., Millo E., Scarfì S., Usai C., Sturla L., Palombo D., De Flora A., Zocchi E. (2009). Abscisic acid released by human monocytes activates monocytes and vascular smooth muscle cell responses involved in atherogenesis. J Biol Chem. 26;284(26):17808-18

Magnone M., Sturla L., Jacchetti E., Scarfì S., Bruzzone S., Usai C., Guida L., Salis A., Damonte G., De Flora A., Zocchi E. (2012). Autocrine abscisic acid plays a key role in quartz-induced macrophage activation. FASEB J. 26(3):1261-71

Magnone M., Ameri P., Salis A., Andraghetti G., Emionite L., Murialdo G., De Flora A., and Zocchi E. (2015). Microgram amounts of abscisic acid in fruit extracts improve glucose tolerance and reduce insulinemia in rats and in humans. FASEB J.; 29:4783-4793

Magnone M., Leoncini G., Vigliarolo T., Emionite L., Sturla L., Zocchi E., Murialdo G. (2018). Chronic Intake of Micrograms of Abscisic Acid Improves Glycemia and Lipidemia in a Human Study and in High-Glucose Fed Mice. Nutrients. 12;10(10):1495

Magnone M., Emionite L., Guida L., Vigliarolo T., Sturla L., Spinelli S., Buschiazzo A., Marini C., Sambuceti G., De Flora A., Orengo A.M., Cossu V., Ferrando S., Barbieri O., Zocchi E. (2020). Insulin-independent

stimulation of skeletal muscle glucose uptake by low-dose abscisic acid via AMPK activation. Sci. Rep.; 29;10(1):1454

Magnone M., Sturla L., Guida L., Spinelli S., Begani G., Bruzzone S., Fresia C., Zocchi E. (2020). Abscisic Acid: A Conserved Hormone in Plants and Humans and a Promising Aid to Combat Prediabetes and the Metabolic Syndrome. Nutrients. 12(6):E1724

Magnone M., Spinelli S., Begani G., Guida L., Sturla L., Emionite L., Zocchi E. (2022). Abscisic Acid Improves Insulin Action on Glycemia in Insulin-Deficient Mouse Models of Type 1 Diabetes. Metabolites. 12(6):523

Mayer H., Salzer U., Breuss J., Ziegler S., Marchler-Bauer A., Prohaska R. (1998). Isolation, molecular characterization, and tissue-specific expression of a novel putative G protein coupled receptor. Biochim Biophys Acta. 11;1395(3):301-8

Mayer H., Bauer H., Prohaska R. (2001). Organization and chromosomal localization of the human and mouse genes coding for LanC-like protein 1 (LANCL1). Cytogenet Cell Genet. 93(1-2):100-4

Milborrow B.V. (2001). The pathway of biosynthesis of abscisic acid in vascular plants: a review of the present state of knowledge of ABA biosynthesis. J Exp Bot. 52(359):1145-64

P

Petrocelli J.J, Drummond M.J. (2020). PGC-1a-targeted therapeutic approaches to enhance muscle recovery in aging. Int J Environ Res Public Health. 17(22):8650

Prabhakar P.K., Doble M. (2008). A target based therapeutic approach towards diabetes mellitus using medicinal plants. Curr Diabetes Rev. 4(4):291-308

Prabhakar P.K., Doble M. (2011). Mechanism of action of natural products used in the treatment of diabetes mellitus. Chin J Integr Med. 17(8):563-74

R

Raghavendra A.S., Gonugunta V.K., Christmann A., Grill E. (2010). ABA perception and signalling. Trends Plant Sci. 15(7):395-401

S

Sahl H.G., Bierbaum G. (1998). Lantibiotics: biosynthesis and biological activities of uniquely modified peptides from gram-positive bacteria. Annu Rev Microbiol. 52:41-79

Sanchez-Rangel E., Inzucchi S.E. (2017). Metformin: clinical use in type 2 diabetes. Diabetologia. 60(9):1586-1593

Sarbassov D.D., Guertin D.A., Ali S.M., Sabatini D.M. (2005). Phosphorylation and regulation of Akt/PKB by the rictor-mTOR complex. Science. 18;307(5712):1098-101

Scarfì S., Ferraris C., Fruscione F., Fresia C., Guida L., Bruzzone S., Usai C., Parodi A., Millo E., Salis A., Burastero G., De Flora A., Zocchi E. (2008). Cyclic ADP-ribose-mediated expansion and stimulation of human mesenchymal stem cells by the plant hormone abscisic acid. Stem Cells. 26(11):2855-64

Scarfì S., Fresia C., Ferraris C., Bruzzone S., Fruscione F., Usai C., Benvenuto F., Magnone M., Podestà M., Sturla L., Guida L., Albanesi E., Damonte G., Salis A., De Flora A., Zocchi E. (2009). The plant

hormone abscisic acid stimulates the proliferation of human hemopoietic progenitors through the second messenger cyclic ADP-ribose. Stem Cells. 27(10):2469-77

Spinelli S., Begani G., Guida L., Magnone M., Galante D., D'Arrigo C., Scotti C., Iamele L., De Jonge H., Zocchi E., Sturla L. (2021). LANCL1 binds abscisic acid and stimulates glucose transport and mitochondrial respiration in muscle cells via the AMPK/PGC-1a/Sirt1 pathway. Mol Metab. 53:101263

Sturla L., Fresia C., Guida L., Bruzzone S., Scarfì S., Usai C., Fruscione F., Magnone M., Millo E., Basile G., Grozio A., Jacchetti E., Allegretti M. De Flora A., Zocchi E. (2009). LANCL2 is necessary for abscisic acid binding and signaling in human granulocytes and in rat insulinoma cells. J Biol Chem. 9;284(41):28045-28057

Sturla L., Fresia C., Guida L., Grozio A., Vigliarolo T., Mannino E., Millo E., Bagnasco L., Bruzzone S., De Flora A., Zocchi E. (2011). Binding of abscisic acid to human LANCL2. Biochem Biophys Res Commun. 18;415(2):390-5

Sturla L., Mannino E., Scarfì S., Bruzzone S., Magnone M., Sociali G., Booz V., Guida L., Vigliarolo T., Fresia C., Emionite L., Buschiazzo A., Marini C., Sambuceti G., De Flora A., Zocchi E. (2017). Abscisic acid enhances glucose disposal and induces brown fat activity in adipocytes in vitro and in vivo. Biochim Biophys Acta Mol Cell Biol Lipids. 1862(2):131-144

T

Tan Y., Zhang Z., Zheng C., Wintergerst K.A, Keller B.B., Cai, L. Mechanisms of diabetic cardiomyopathy and potential therapeutic strategies: preclinical and clinical evidence. (2020). Nat Rev Cardiol. 17(9):585-607.

Tang J., Lu L., Liu Y., Ma J., Yang L., Li L. (2019). Quercetin improves ischemia/reperfusion-induced cardiomyocyte apoptosis in vitro and in vivo study via SIRT1/PGC-1a signalling. Journal of Cellular Biochemistry 120:9747e9757

Tian L., Cao W., Yue R., Yuan Y., Guo X., Qin D., Xing J., Wang X. Pretreatment with Tilianin improves mitochondrial energy metabolism and oxidative stress in rats with myocardial ischemia/reperfusion injury via AMPK/SIRT1/PGC-1 alpha signaling pathway. (2019). J Pharmacol Sci. 139(4):352-360.

Tossi V., Cassia R., Bruzzone S., Zocchi E., Lamattina L. (2012). ABA says NO to UV-B: a universal response? Trends Plant Sci. 17(9):510-7

V

Vigliarolo T., Guida L., Millo E., Fresia C., Turco E., De Flora A., Zocchi E. Abscisic acid transport in human erythrocytes. (2015). J Biol Chem. 22;290(21):13042-52.

W

Walker M.C., Eslami S.M., Hetrick K.J., Ackenhusen S.E., Mitchell D.A., van der Donk W.A. (2020). Precursor peptide-targeted mining of more than one hundred thousand genomes expands the lanthipeptide natural product family. BMC Genomics. 3;21(1):387

Wu Y., Kuzma J., Maréchal E., Graeff R., Lee H.C., Foster R., Chua N.H. (1997). Abscisic acid signaling through cyclic ADP-ribose in plants. Science. 19;278(5346):2126-30

Wu Y., Ding Y., Tanaka Y., Zhang W. (2014). Risk factors contributing to type 2 diabetes and recent advances in the treatment and prevention. Int J Med Sci. 6;11(11):1185-200

www.WHO.int
www.diabetes.org
www.proteinatlas.org

Y

Yoon Y., Seo D.H., Shin H., Kim H.J., Kim C.M., Jang G. (2020). The Role of Stress-Responsive Transcription Factors in Modulating Abiotic Stress Tolerance in Plants. Agronomy.

Yu A., Zhou R., Xia B., Dang W., Yang Z., Chen X. (2020). NAMPT maintains mitochondria content via NRF2-PPARa-/AMPKa pathway to promote cell survival under oxidative stress. Cell Signal. 66:109496

Z

Zamboni F., Cengiz I.F., Barbosa A.M., Castro A.G., Reis R.L., Oliveira J.M., Collins M.N. (2021). Towards the development of a female animal model of T1DM using hyaluronic acid nanocoated cell transplantation: refinements and considerations for future protocols. Pharmaceutics. 13(11):1925

Zeng M., van der Donk W.A., Chen J. (2014). Lanthionine synthetase C-like protein 2 (LanCL2) is a novel regulator of Akt. Mol Biol Cell. 1;25(24):3954-61

Zhang J., He, Z., Fedorova J., Logan C., Bates L., Davitt K., Le V., Murphy J., Li M., Wang M., Lakatta E.G., Ren D., Li J. Alterations in mitochondrial dynamics with age-related Sirtuin1/Sirtuin3 deficiency impair cardiomyocyte contractility. Aging Cell 2021, 20(7):e13419.

Zocchi E., Hontecillas R., Leber A., Einerhand A., Carbo A., Bruzzone S., Tubau-Juni N., Philipson N., Zoccoli-Rodriguez V., Sturla L., Bassaganya-Riera J. (2017). Abscisic acid: a novel nutraceutical for glycemic control. Front. Nutr. 13;4:24.

ACKNOWLEDGEMENTS

I don't know where my road is going, but I know that I walk better when I hold your hand. (Alfred de Musset)

Every barrier, every difficulty can be overcome when you're surrounded by great and amazing people.

First, I want to thank *my mother Antonella and my father Maurizio*. They deserve much more than these short lines written here, but it's just a small sign of gratitude for them. They know me as nobody else and have always supported me from my first steps until now that I've grown up. They are the cornerstone of my life, they made lots of sacrifices for me, helping me to realize myself and my dreams and I can't thank them enough for this.

Then, I want to thank *my sister Laura* for her irreplaceable and invaluable love. She is one of the most important people in my life and she, like no one else, can understand how much difficult and hard this road is. We have always shared everything, and I've always known how much she was worth. I'm so proud of her because she followed in my footsteps becoming a biotechnologist. I'm sure she will always be able to deal with the difficulties of life because she is a rock, and I will always be there for her. I hope that she can obtain everything she want from life and I'm sure that she will be a great person and scientist.

A big thank to *my aunt Paola*: she is like a shadow, always behind me to support and sustain me.

A huge thank goes to *my grandmothers Carla and Emilia*, *my uncles Danilo and Vincenzo* and *my aunt Sandra*: even if we can't

see each other so much, they are always in my mind and my thoughts (along with *my three guardian angels Mario, Patrizia and Virginio*) and I love all of you to the moon and back.

Now, it's time to special thanks to *Danilo*. He came into my life out of the blue in a particular moment of my life, when I was upset, and I quickly realize how much he was worth. We share Life since 2019 and, even not understanding this world, he has never hindered me, and he has waited for me for three years. Life has already put us to the test, but we didn't give up, and now we are still here, ready for another challenge. He taught me the meaning of growing strong due to the sufferings that Life puts in front of you, but he also taught me how to always believe in myself, how to be self-confident, how to love myself just the way I am and now I can't wait to continue to walk with him for the rest of my life, I hope.

Besides, a huge thank also goes to *my "father-in-law" Giovanni*. He has always been by my side since the moment we met, and it's not obvious.

Since 2019 I was lucky enough to discover the wonderful world of Red Cross volunteering. I must thank my travel companion, who were able to stay close to me for these three years. First, the components of Local Operation Room *Adriano, Marinella, Nicola and Patrizio*: share and dialogue with them allowed me to grow and mature a lot.

Besides, I want to thank *Federica and Silvia*, always there to share their huge and beautiful smile.

Thanks also to *all the Volunteers* who relieve my burden of distance even just with a smile or a word.

After that, a huge thank to *Pino Palmieri*: I had the honor of meeting him in 2019 and working by his side for 3 years. Unfortunately, he passed away a year ago, but even now I carry with me his teachings and lessons: he taught me to go everywhere on tiptoe, to be sure of what I am and to work in team for the good of Red Cross of Bra, which he loved until the last day on this Earth and, above all, to be always on the side of more vulnerable and less fortunate people.

Many thanks also to all my colleagues from Biochemistry section, *Andrea, Cecilia, Elena, Francesco, Lucrezia, Maria Elena, Mirko, Santina and Sonia* for sharing these three years.

Thank you *Rosy*, my favorite scientist, because we shared all of our joys and sorrows and we supported each other constantly; even if I'm not there physically anymore, I love you so much and I will always be available for you.

Last, but not least, I want to thank you *my tutors Elena and Laura* for teaching me how to think and how to approach the research and its problems. Their teachings will never be forgotten.

RINGRAZIAMENTI

Io non so dove andrà la mia strada, ma so che cammino meglio quando mi tenete per mano. (Alfred de Musset)

Ogni barriera e ogni difficoltà può essere superata quando si è circondati da persone meravigliose.

Prima di tutto, vorrei ringraziare *mia mamma Antonella e mio papà Maurizio*. Meritano ben più di queste due brevi righe che scriverò qui, ma questo è solo un piccolo gesto di gratitudine nei loro confronti. Loro mi conoscono meglio di chiunque altro e mi hanno sempre supportato, dai miei primi passi fino ad ora che sono un'adulta. Sono il pilastro della mia vita, hanno fatto tantissimi sacrifici per me, aiutandomi a realizzarmi e a realizzare i miei sogni e per questo non potrò mai ringraziarli abbastanza.

Ringrazio poi *mia sorella Laura* per il suo insostituibile affetto. È una delle persone più importanti della mia vita e lei, come nessun altro, può capire quanto difficile e dura questa strada sia. Abbiamo sempre condiviso tutto, e io ho sempre saputo quanto valesse. Sono veramente orgogliosa di lei, perché ha seguito le mie orme diventando una biotecnologa. Sono certa che sarà sempre in grado di fronteggiare tutte le difficoltà che la vita le presenterà perché lei è una roccia, e sa che io sarò sempre al suo fianco. Spero che riesca e possa ottenere qualsiasi cosa voglia dalla vita e sono sicura che sarà una persona meravigliosa e una grande ricercatrice.

Un enorme ringraziamento a mia zia Paola: lei è come un'ombra, sempre dietro di me a supportarmi e sostenermi.

Un grande ringraziamento va alle *mie nonne Emilia e Carla*, *ai miei zii Danilo e Vincenzo* e a *mia zia Sandra* perché anche se la Vita non ci permette di vederci molto spesso, sono sempre nella mia mente e nei miei pensieri (insieme *con i miei tre angeli custodi Mario, Patrizia e Virginio* che amo con tutto il cuore).

Ora, è tempo per un ringraziamento speciale a *Danilo*. Lui è entrato nella mia vita come un fulmine a ciel sereno, in un momento in cui ero triste, e mi sono resa conto in poco tempo quanto valesse la pena approfondire la sua conoscenza. Noi condividiamo la Vita dal 2019 e, anche se non ha mai compreso fino in fondo il mondo della ricerca, non mi ha mai ostacolato e soprattutto mi ha aspettato per tre anni. La vita ci ha già messo alla prova, ma noi non abbiamo mollato e siamo ancora qui, pronti per la prossima sfida. Mi ha insegnato cosa vuol dire crescere forti a causa del dolore che la Vita ti mette davanti, ma mi ha anche insegnato a credere sempre in me stessa, ad essere sicura di ciò che sono, ad amarmi per quello sono e adesso non vedo l'ora di continuare a camminare fianco a fianco con lui per il resto della mia Vita.

Poi, un enorme ringraziamento va a "*mio suocero*" *Giovanni*. Lui è stato dalla mia parte dal momento in cui ci siamo incontrati la prima volta, e non è una cosa così scontata.

Dal 2019, ho avuto la fortuna di scoprire il mondo del volontariato della Croce Rossa. Un ringraziamento doveroso ai miei compagni di viaggio che sono stati capaci di stare al mio fianco per tre anni. Prima di tutto, i componenti della Sala Operativa Locale *Adriano, Marinella, Nicola e Patrizio*: la condivisione e il confronto mi hanno permesso di crescere e maturare tanto.

Inoltre, voglio ringraziare *Federica e Silvia*, sempre presenti per condividere un abbraccio o un meraviglioso sorriso.

Un ringraziamento va anche a *tutti i Volontari* che anche solo con un sorriso o una parola hanno alleviato il peso della lontananza per tre anni.

A seguire, un enorme ringraziamento a *Pino Palmieri*: ho avuto l'onore di conoscerlo nel 2019 e lavorare al suo fianco per tre anni. Purtroppo, è mancato da un anno circa, ma ancora oggi porto con me i suoi insegnamenti e le sue lezioni di vita: arrivare dovunque in punta di piedi, essere sicuri di ciò che si è e lavorare sempre come una squadra per il bene della Croce Rossa di Bra, che lui ha amato fino all'ultimo giorno su questa Terra e, soprattutto, stare sempre dalla parte degli ultimi.

Un ringraziamento ai miei colleghi della sezione di Biochimica *Andrea, Cecilia, Elena, Francesco, Lucrezia, Maria Elena, Mirko, Santina, Sonia* per aver condiviso questi tre anni.

Un ringraziamento grande anche a *Rosy*, la mia scienziata preferita, per aver condiviso con me tutte le gioie e i dolori. Ci siamo supportate costantemente e anche se non sarò lì fisicamente, ti voglio tanto bene e sarò sempre disponibile per te.

Ultimo, ma non meno importante, vorrei ringraziare *Elena e Laura* per avermi insegnato come pensare e come approcciare la ricerca e i suoi problemi. I loro insegnamenti non andranno mai dimenticati.